

C.P. No. 518
(18,247)
A.R.C. Technical Report

C.P. No. 518
(18,247)
A.R.C. Technical Report

LIBRARY
ROYAL AIRCRAFT ESTABLISHMENT
BEDFORD.



MINISTRY OF AVIATION
AERONAUTICAL RESEARCH COUNCIL
CURRENT PAPERS

Some Tests on an Avon-Canberra Installation to Measure Thrust in Flight

By

R. Holl, R.G. Lea and Sqn.Ldr. J.E. Boden

LONDON: HER MAJESTY'S STATIONERY OFFICE

1960

SIX SHILLINGS NET

June, 1955.

NATIONAL GAS TURBINE ESTABLISHMENT

Some tests on an Avon-Canberra installation
to measure thrust in flight

- by -

R. Holl, R. G. Lea and Sqn.Ldr. J. L. Boden, R.A.F.

SUMMARY

Three aerodynamic methods of thrust measurement have been investigated:-

- (i) The "standard" single pitot method.
- (ii) The use of a jet pipe pitot pressure rake.
- (iii) The use of a pitot-static pressure rake at the plane of the final nozzle.

The results of the tests indicate that the accuracy of the single pitot method was of the order of ± 3 per cent but that this technique could be improved by the use of a pitot pressure rake with which an accuracy of $\pm 1\frac{1}{2}$ per cent was indicated. There was consistently good agreement between the thrust readings obtained by the jet pipe pitot rake and the pitot-static pressure rake at the final nozzle. There is little to choose between the two rake methods, the pitot-static rake has the advantage that no bench calibration of the engine is essential once the drag characteristics of the rake form are established, but it is more complicated and more difficult to install than a jet pipe rake.

Further flight tests are required to investigate the scatter of experimental results which did occur and to obtain a more accurate assessment of the thrust performance of the engine at high altitudes.

CONTENTS

	<u>Page</u>
1.0 Introduction	5
2.0 Instrumentation	6
2.1 The intake rake	6
2.2 The jet pipe rake	6
2.3 The final nozzle rake	6
2.4 Automatic observers	7
3.0 Test procedure	7
3.1 The ground calibration	7
3.2 Flight tests	7
3.3 Some operational problems	8
4.0 Test results	9
4.1 Ground calibration	9
4.2 Flight results	9
5.0 Discussion of results	9
5.1 Gross thrust values	9
5.2 Final nozzle static pressure distribution	10
5.3 Engine performance	11
6.0 Conclusions and recommendations	12
Acknowledgment	13
References	14
List of symbols	15

TABLES

<u>No.</u>	<u>Title</u>	
I	Calculation of thrust and mass flow from final nozzle rake	18
II	Calculation of thrust and mass flow from jet pipe rake	19

APPENDICES

<u>No.</u>	<u>Title</u>	
I	List of measuring points and associated instruments	16
II	Determination of gross thrust	17

APPENDICES (cont'd.)

<u>No.</u>	<u>Title</u>	<u>Page</u>
III	Derivation of ambient temperature and pressure	20
IV	Discharge from a jet pipe	22

ILLUSTRATIONS

<u>Plate No.</u>	<u>Title</u>
Plate 1	Final nozzle pressure rake
Plate 2	Final nozzle rake after flight tests
Plate 3	Front rake after removal and repair
Plate 4	Rear rake after removal and repair

<u>Fig. No.</u>	<u>Title</u>
1	Arrangement of rakes in jet pipe
2	Diagrammatic representation of speeds and altitudes covered during flight trials
3	Typical pressure distribution across final nozzle. Test bed results.
4	Test bed measured thrust and calculated rear rake thrust
5	Effective area calibration curves
6	Typical thrust versus rev/min curves obtained during flight trials
7	Single pitot effective area computed from flight results
8	Static pressure distribution across final nozzle
9	Contour lines of static pressure in horizontal plane through final nozzle. Derwent V engine No.3456, corrected speed 14,750 rev/min.
10	Centre static pressure ratio versus overall nozzle pressure ratio
11	Thrust versus altitude chart
12	Non-dimensional plot of thrust versus rev/min showing correlation of theoretical figures to actual results

ILLUSTRATIONS (cont'd.)

<u>Fig. No.</u>	<u>Title</u>
13	Jet pipe temperature versus altitude
14	Actual nozzle pressure ratio versus overall nozzle pressure ratio

1.0 Introduction

An extensive series of tests to investigate the pitot rake method of measurement of jet engine thrust in flight has been carried out by A. and A.E.E., Boscombe Down, using a Derwent engine installed in a Meteor 4 aircraft, and they are fully reported in Reference 1. In the final paragraph of this Report it is recommended that further tests should be made with a pitot-static rake fitted to another engine type, preferably with an axial compressor.

Further flight tests have now been carried out and the following Report describes the first series of tests on an Avon R.A.3 engine installed in a Canberra aircraft.

The significant conclusions of Reference 1 were:-

- (a) Changes in jet pipe total pressure distribution between test bed and flight conditions result in single pitot sampling errors of up to 3 per cent in total head pressure, equivalent to 5 per cent in thrust.
- (b) To make an absolute measurement of thrust by the momentum method it will be necessary to use a pitot-static rake (not a pitot rake) at the plane of the final nozzle.

It was therefore decided that the Avon installation should feature the following equipment in order to gain further knowledge of the aerodynamic methods of thrust measurement:-

- (a) A "standard" single pitot tube as installed for the normal method of thrust measurement².
- (b) A pitot rake carrying a multiplicity of pitot pressure tubes and total temperature thermocouples, this being an improvement on the standard single pitot and four thermocouple equipment in that it would be less sensitive to local variations of jet pipe total pressure and temperature.
- (c) A pitot-static pressure measuring rake at the plane of the final nozzle.

The aircraft installation was also equipped with hydraulic force measuring elements at the engine trunnions for direct thrust measurements, but mechanical difficulties associated with the free movement of the engine were experienced and this method of thrust measurement was temporarily abandoned in order to carry out tests with the jet pipe equipment.

2.0 Instrumentation

The engine used for the tests was a Rolls-Royce Avon R.A.3 type (Serial No. 291) and it was installed in the starboard nacelle of a Canberra B.2 aircraft (Serial No. WH.657).

The rear section of a standard jet pipe was removed and replaced by one carrying the two measuring rakes. In addition to the extensive

instrumentation of the jet pipe, care was taken to obtain accurate measurements of compressor intake pressure, fuel flow, compressor delivery pressure and other normal engine performance readings. Some 90 individual pressure and temperature tapings were connected to the appropriate indicators mounted in six automatic observers in the bomb bay of the aircraft. The remote operation of the observers was from a control box in the cockpit. The individual measuring points are listed as Appendix I together with the details of the various types of indicator used. A more detailed description of some of the instrumentation equipment is given below:-

2.1 The intake rake

The compressor inlet total pressure was measured by nine individual pitot tubes located in the leading edge of one of the streamlined front bearing supports of the compressor intake. The tubes were of 2 m/m steel hypodermic tubing and located to relate to equal annular areas.

2.2 The jet pipe rake

As a refinement of the single pitot arrangement, a jet pipe rake was made to measure both total temperature and total pressure at a number of points across the diameter of the jet pipe. Twelve total pressure tubes of 2 m/m hypodermic tubing were located along the leading edge of a streamlined fairing and interspaced between them were twelve radiation shielded total temperature thermocouples. Both the thermocouples and pitot tubes were disposed to relate to equal annular areas of the jet pipe. A diagrammatic arrangement is shown in Figure 1. For bench tests without this rake, profiled plates were made to blank off the holes in the jet pipe wall in which the rake was located. Plate 3 shows the rake with its twelve pressure tubes and twelve thermocouples before installation in the jet pipe. The individual pressures were measured on -3 to +20 lb/sq.in. differential pressure gauges, the remaining gauge tapings being connected to the aircraft static pressure tapping. The thermocouples were connected to 0 to 700°C jet pipe temperature indicators.

It was thought that such a multi-point arrangement of temperature and pressure measurement would be less susceptible than single point measurements to variations in radial pressure and temperature distribution and to the random fluctuations which occur in the jet stream.

2.3 The final nozzle rake

A detachable pitot-static pressure measuring rake was designed to measure the pressure distribution at the plane of the final nozzle. The rake consisted of a streamlined strut fixed by two outriggers to the final nozzle flange. Plate 1 shows this rake following completion of the ground calibration of the engine, whilst Plate 2 shows it as installed for the flight tests. It will be noted that the nozzle flange has been considerably reduced. This was necessary to restore a satisfactory cooling airflow through the engine nacelle. Plate 4 shows the rake assembly before installation. The individual pitot and static tubes are of 2 m/m and 3/16 in. O.D. stainless steel tubing respectively and are disposed to read mean pressures for equal flow areas.

2.4 Automatic observers

The various instruments were contained in six automatic observers, five in the bomb bay and one in the rear camera position. Each observer was equipped with an F-73 type camera. Operation of the observers was by a press button in the cockpit. To obviate a sudden heavy loading of the electrical system the observer lights were sequentially switched by relays and then the cameras operated simultaneously.

3.0 Test procedure

The work was carried out in two distinct complementary phases, the ground calibration and the subsequent flight tests. On the test bed a precimeter was used to measure thrust, jet pipe pressures were measured on manometers, and jet pipe temperatures were recorded by a multi-point indicator.

3.1 The ground calibration

The engine was fitted with a Rolls-Royce type of test-bed intake flare designed to give an effectively radial flow into the engine.

It was run at speeds from 6,200 rev/min to governed rev/min. Performance readings were taken at intervals during this running and the engine was run with the following combinations:-

1. No rakes fitted.
2. Jet pipe rake only fitted.
3. Final nozzle rake only fitted.
4. Both rakes fitted.

Finally a two hour acceptance test to clear the engine for flight use was run during which performance readings were again taken. This proof test was run with both rakes fitted.

3.2 Flight tests

For the initial flight tests an indicated air speed (I.A.S.) in level flight of 280 knots was selected. This enabled a range of engine speeds to be selected on the test engine at altitudes up to 32,000 ft, whilst this constant I.A.S. was maintained by suitable control of the port engine. Further flights were carried out to extend the range of altitudes and I.A.S. Figure 2 shows diagrammatically the range of I.A.S. and altitude which have been covered. This represents ram ratios in the range from 1.074 to 1.51 at altitudes from 400 to 45,000 ft. All flights were carried out with a pre-flight altimeter setting of 1,013.2 mbs.

During readings the aircraft was flown at constant I.A.S. and altitude whilst both engines were varied in speed to maintain this flight condition. The test engine was operated over the rev/min range from 6,600 rev/min to 7,800 rev/min. The latter represents maximum take-off and operational necessity rev/min. The lower rev/min was chosen since it was above the operating rev/min for the intake vanes and bleed valves and was considered low enough to ensure that the final nozzle was not choked at low ram ratios.

At each engine rev/min the camera button was operated three times with an interval of some five seconds between each operation. This gave three pictures at each engine condition from which mean values were obtained.

Readings were taken with the test engine increasing in rev/min in order to minimise any effects of instrument lag or stiction. This was possible only up to approximately 35,000 ft. Above this it was necessary to obtain the reading required quickly and then to throttle back to prevent overheating in the engine nacelle.

3.3 Some operational problems

The aim during testing was to maintain the aircraft at a constant I.A.S. within ± 2 knots and at a constant altitude within ± 50 ft. Flying to these fine limits was generally achieved, but the task became more difficult in turbulent air and as altitude increased.

During ground running after the installation of the modified jet pipe in the aircraft, overheating occurred in the engine nacelle resulting in destruction of the flexible synthetic rubber tubes connecting rake pressure tubes to the aircraft piping system. This overheating was attributed mainly to the interference with the jet pipe cooling air stream ejector by the flange at the end of the jet pipe, and partly due to blockage of the nacelle area by the instrumentation.

It was decided to restore the external profile of the end of the jet pipe to the original shape except where the rear rake mounting prevented this. This modification which meant cutting away most of the rear flange prevented any re-positioning of the rake which was the original purpose of the complete multi-hole flange. Also, the aircraft instrument piping system was lengthened thus shortening the flexible rubber pipes. As a further precaution silicone rubber tubing replaced the original synthetic rubber. Subsequent ground running indicated satisfactory engine compartment cooling, and satisfactory flight testing was possible up to an altitude of 25,000 ft. Above this altitude overheating occurred and a resistance type temperature bulb was fitted inside the jet pipe cone fairing adjacent to the rubber tubes with its indicator situated in the pilot's cabin. By reference to this instrument it was possible to obtain some performance readings up to 45,000 ft by judicious use of the test engine throttle when the gauge showed an increase from its normal reading.

Some difficulty was experienced toward the end of the trials with the observer cameras. Jamming of the film in the cassettes was found to be the cause and careful selection of the cassettes was a solution. Failure of one camera occurred during the flight test period.

During flights on which readings were obtained over a range of altitudes it was necessary to obtain readings at ascending heights as with the reverse procedure condensation on the camera lenses occurred resulting in blurring of the observer records.

4.0 Test results

Since the testing occurred in two phases it is convenient to consider the results in the same way and the results of the ground calibration and the flight tests are considered separately below.

4.1 Ground calibration

As stated previously, ground performance calibration of the engine was carried out over the higher speed range and with no rakes fitted, with each rake fitted individually and with both rakes³. For all tests readings from the standard four jet pipe thermocouples and the normal single jet pipe pitot tube were recorded. It was originally intended to obtain flight results with single rakes operating but within the time available it was only possible to complete a flight series with both rakes fitted and this was the main feature of the engine arrangement tested both on the ground and in flight.

The thrust of the engine was calculated from the final nozzle rake pressures and compared with the measured thrust. The form of the pressure distribution at the final nozzle is shown in Figure 3. Figure 4 shows a typical plot of thrust curves obtained by the two methods. Accepting the test bed thrust measurement as the basic engine performance the scatter of the computed thrust measurements was between limits of accuracy from -1.6 per cent to +1.4 per cent. The test bed results plotted in the form of an effective nozzle area against overall pressure ratio are shown on Figure 5.

At a maximum engine speed (7,900 rev/min) the drag of the rear rake was estimated from the performance figures with and without the rake fitted and found to be 120 lb, and it was assumed to vary as ρV_j^2 at lower jet velocities³.

4.2 Flight results

The range of flight testing was from 400 ft to 40,000 ft and extended over the ram ratio range from 1.07 to 1.51. Over this range the agreement between the thrust values as measured by the jet pipe rake ("front rake") and the final nozzle rake ("rear rake") was good and generally within 1 per cent although a few random points upset the claim that this limit of agreement was absolute. Figure 6 shows a typical set of results. Separate curves of gross thrust have been drawn for each of the methods used and it will be noted that at most altitudes a single line could well have been drawn through the points from the two rakes.

The thrust figures from the single pitot are not so consistent but nevertheless show better agreement than was experienced during the earlier tests¹ on the Derwent engine.

5.0 Discussion of results

The following are the major points arising from an examination of the test results:-

5.1 Gross thrust values

As mentioned earlier, the agreement between gross thrust values computed from the readings of the two rakes was good over the whole test range. The values computed from the single pitot readings also showed fair agreement. If it is assumed that at any flight condition the true gross thrust is the mean of the values obtained by the two rakes then values of A_f (effective final nozzle area) can be computed from the corresponding single pitot readings. Such calculations have been done

and the results are presented as Figure 7. The extent of the scatter of the individual values of Af is a measure of the accuracy not only of the single pitot method but also of the rake method of determining thrust. Whilst these two sources of error cannot be separated the rear rake method is an absolute measure of thrust and showed an accuracy of 1½ per cent during ground tests. From Figure 7 it is clear that, except for a few isolated points, the use of the single pitot method allied with the ground calibration curve for Af would result in errors of only about 2 or 3 per cent at the most. This is considerably better than the 5 or 6 per cent accuracy for the single pitot method as concluded in Reference 1. When one considers the difference between the Derwent and Avon installations this is understandable because:-

- (a) The Avon has a two stage turbine and a lower turbine outlet gas velocity and hence a more even gas velocity distribution at entry to the exhaust system.
- (b) There is less outlet swirl of the gas leaving the Avon turbine than in the case of the Derwent, thus giving less change of pitot position error.
- (c) The area changes in the exhaust system are more even and the jet pipe is longer, both features helping to give a more even velocity distribution at the measuring stations.

An examination of all the flight results shows that scatter of the experimental points increases with altitude and in agreement with the findings of Reference 1 it would be an advantage to use lower range pressure gauges for these readings.

5.2 Final nozzle static pressure distribution

An interesting feature of the test results was the level and distribution of static pressure across the plane of the final nozzle measured both on the test bed (Figure 3) and in flight as shown in Figure 8. It will be noted that the distribution is approximately elliptical. Similar results have been obtained by Deacon⁴ during tests on a Derwent engine and more recently by Rolls-Royce⁵ on Avon engines particularly the R.A.7 engine in the Hunter. The form of the static pressure distribution in the region of the plane of the final nozzle for a Derwent engine has been extracted from Reference 3 and presented as Figure 9. The significant level of static pressure and its distribution across the plane of the final nozzle is commented on in Reference 3 and is the main reason for the recommendation by the authors that a pitot rake is inadequate to give an absolute measure of thrust and must be backed by static pressure measurements.

Three dimensional theory predicts that there is a slight rise in static pressure at the centre of the plane of an unchoked convergent nozzle, and that the distribution across the plane is similar to that measured, but the predicted level of static pressure is insignificant compared with the measured values. Figure 10 shows how the centre static pressure varies with increasing overall nozzle pressure ratio together with the static pressure variation as predicted by one-dimensional flow theory*, and it will be noted that the curves have a similar slope.

*This states that the static pressure distribution across the plane of the nozzle is uniform and equal to ambient pressure until the nozzle is choked. After this it becomes equal to

$$\frac{P_{St}}{\left(\frac{\gamma-1}{2}\right)^{\frac{\gamma}{\gamma-1}}}$$

In Appendix IV an attempt has been made to explain the high values of static pressure based on the assumption that the effective throat of the nozzle is downstream of the physical throat.

5.3 Engine performance

The thrust performance of the engine is shown on Figure 11 corrected to I.C.A.N. conditions for a constant I.A.S. of 280 knots up to an altitude of 30,000 ft. Except for some bad scatter of the points for the thrust at lowest engine speed, the remaining values are consistent and indicate the good agreement between the experimental methods. In those instances where the individual values agree for one test condition but give scatter when associated with other groups of points then the fault would appear to be with the measurement of corrected engine speed.

The usual non-dimensional theory states that the non-dimensional thrust is a function only of corrected engine speed $\left(\frac{N}{\sqrt{T}}\right)$ and the ram ratio $\left(\frac{P_{t1}}{P_a}\right)$. In order to compare the gross thrust of an engine in flight over a range of $\frac{N}{\sqrt{T}}$ at several ram ratios, some function of gross thrust independent of ram ratio and varying only with $\frac{N}{\sqrt{T}}$ is required.

It can be shown that when the final nozzle is choked then the function

$$\frac{\frac{F_G}{A_f P_a} + 1}{R_{a1}}$$

should lie on a unique curve if the assumptions of the non-dimensional theory are correct. With the final nozzle not choked measurements at a selected ram ratio should be on unique curves. Figure 12 shows the thrust performance of the Avon engine presented in this form taken from the firm's brochure together with points calculated from the actual thrust values obtained during the flight tests. The same value of $A_f (= 299)$ as used for the brochure curves was used to calculate the values of

$$\frac{\frac{F_G}{A_f P_a} + 1}{R_{a1}}$$

At this stage it should be stated that the ram ratio values used for the calculated points were those actually obtained from the engine compressor intake pitot rake. These showed practically an even distribution across the whole intake, the mean pressure varying an almost negligible amount from the corresponding A.S.I. total head pressure indication. There are insufficient experimental points and the random values of ram ratio prevent any clear deductions being made. There is, however, an indication that the distribution of the points is related to a unique set of curves of a similar form to the predicted curves but lying slightly below and falling off more decidedly at the higher values of $\frac{N}{\sqrt{T}}$.

Because of the limitations imposed due to overheating in the engine nacelle performance readings were not obtained above 45,000 ft. The few readings that were obtained at the higher altitude do indicate a possible effect of Reynolds number on the engine performance. Jet pipe temperature values have been plotted for constant values of $\frac{N}{\sqrt{T}}$ and it will be noted in Figure 13 that the curves are rising steeply at approximately 40,000 ft. It has been noted⁶ that when the value of $T_{st}/T_{1,t}$ reaches that measured under sea level static conditions then a deterioration in performance occurs which can be attributed to a reduction in Reynolds number.

6.0 Conclusions and recommendations

It is considered that further tests are required before the whole of the limitations and accuracy of the aerodynamic methods of thrust measurement in flight can be determined. However, the following conclusions seem warranted:-

6.1 The accuracy of thrust measurement by the single pitot method is considerably improved in the case of the Avon engine as installed in the Canberra when compared with the results from the Derwent-Meteor installation. Generally, the errors do not exceed 3 per cent.

6.2 At altitudes up to 25,000 ft, the use of a pitot-static rake gives consistent values of absolute thrust with little more than ± 1 per cent scatter of the experimental points.

6.3 The use of a pitot pressure rake is a big improvement over the use of a single pitot, an accuracy of ± 1.5 per cent is indicated and its use is recommended. There appears to be no need to increase the number of jet pipe total temperature thermocouples from the standard four normally fitted as there was consistently good agreement between their readings and those of the twelve thermocouples on the jet pipe rake.

The following recommendations are made:-

6.4 Further flight tests are necessary particularly at selected ram ratios over as wide a range of $\frac{N}{\sqrt{T}}$ as possible.

6.5 The use of lower range multi-turn pressure gauges for jet pipe pressure readings at the higher altitudes is required to maintain accuracy.

6.6 Some form of speed counter to give a calibration of the rev/min indicator under engine operating conditions would be of considerable benefit.

6.7 The integration of the rake readings by feeding them to a common gauge should be investigated, earlier bench tests have indicated that a true arithmetic mean pressure is obtained in this way.

6.8 In order to increase further the accuracy of the readings at the higher altitudes further knowledge of the recovery factor of the air temperature bulb on the aircraft is required, and future flight programme should include some tests to achieve this.

Acknowledgment

The authors wish to express their thanks for the large amount of film reading and computing work carried out by Miss S. Wareham.

REFERENCES

<u>No.</u>	<u>Author(s)</u>	<u>Title, etc.</u>
1	Flt. Lt. Stephenson, R. T. Shields and D. W. Bottle	An investigation into the pitot-rake method of measuring turbo-jet engine thrust in flight. C.P.143, December, 1952.
2	D. J. Higton, R. H. Plascott and D. A. Clarke	Measurement of overall drag of an aircraft at high Mach numbers. R. and M. 2748, January, 1949.
3	K. R. F. Kenworthy R. G. Lea	Unpublished work at N.G.T.E.
4	W. Deacon	Unpublished work at N.G.T.E.
5		Unpublished work by Rolls Royce Flight Development Department, Hucknall.
6	D. W. Thomas	Unpublished work at N.G.T.E.

List of Symbols

A	=	nozzle area
C _p	=	specific heat at constant pressure
F	=	thrust
F ¹	=	rake calculated thrust (excludes rake drag)
g	=	acceleration due to gravity
J	=	heat equivalent of work
P	=	absolute pressure
Q	=	air or gas mass flow
q	=	fuel:air ratio
R	=	gas constant
R _{ai}	=	ram ratio
T	=	absolute temperature
t	=	temperature ratio
V	=	velocity
γ	=	ratio of specific heats
ρ	=	density

Suffices

a	refers to ambient conditions
c	refers to a choking condition
f	refers to an effective value
G	refers to a gross value
P	refers to an effect of pressure
t	refers to total head conditions
v	refers to an effect of velocity
1	compressor intake plane
2	compressor outlet plane
3	turbine inlet plane
4	turbine outlet plane
5	jet pipe plane
6	final nozzle plane

APPENDIX I

Thrust measurement in flight

List of measuring points and associated instruments

No.	Item	No. of points	Location	Indicator
1	Compressor inlet static pressure	4	Outside wall of compressor inlet casing	Mk.19A Altimeter range 0-60,000 ft.
2	Compressor inlet total pressure	9	Pitot tubes on leading edge of one bearing support strut	Air speed indicators type 1/1. Range 50-600 knots.
3	Compressor outlet static pressure	1	Outside wall of compressor outlet casing	Pressure gauge type KBB, Type IT-1/3. Range 0-200 lb/in ²
4	Compressor outlet total temperature	1	Thermocouple in compressor outlet casing	Thermocouple indicators. Range 0-350°C
5	Fuel flow	1	Engine main fuel line	Negretti and Zambra Series 1. Range 0-3,500 kg/hr.
6	Fuel temperature	1	Engine main fuel line	Range -50 - +100°C
7	Jet pipe total temperature	4	Jet pipe at points 90° apart	Sangamo Weston type B
8	Jet pipe total pressure	1	Pitot tube at $\frac{3}{4}$ radius of jet pipe	Pressure gauge, type KBB. IT-1/10. -3 - +20 lb/in ²
9	Jet pipe total temperature	12	Shielded thermocouples in jet pipe rake	Sangamo Weston. Range 0-700°C
10	Jet pipe total pressure	12	Pitot tubes in jet pipe rake	Pressure gauge type KBB IT-1/10. Range -3 - +20 lb/in ²
11	Final nozzle total pressure	12	Pitot tubes in final nozzle rake	Pressure gauge type KBB IT-1/10. Range -3 +20 lb/in ²
12	Final nozzle static pressure	12	Static tubes in final nozzle rake	Pressure gauge type KBB IT-1/10. Range -3 - +20 lb/in ²
13	Nacelle static pressure	12	Static tubes 3 around engine and 4 around jet pipe	Mk.19A Altimeter. Range 0-60,000 ft
14	Nacelle total temperature	1	Adjacent flexible synthetic rubber tubing	Temperature indicator. Range -40 - +140°C
15	Trunnion thrust	4	Engine trunnions 2 forward and 2 aft	Statimeter pressure gauges calibrated in lb. Range 0-6,000 lb
16	Altitude	1		Mk.19A Altimeter. Range 0-60,000 ft
17	Air speed	1		Kollsman type F.1. Range 50-600 m.p.h.
18	Engine rev/min	1	Engine gear box	Mk.10A. Range 0. 20,000 rev/min
19	Ambient air temperature	1	Impact bulb on aircraft nose	Temperature indicators. Range -70 - +30°C

Appendix II

Thrust measurement in flight

Determination of gross thrust

1. With the rear rakes

The gross thrust of an engine is given by

$$F_G = \int \frac{\rho V^2 \delta A}{g} + \int (P_c - P_a) \delta A \quad \dots (1)$$

If however a number of readings are taken in such a manner that they are weighted for area the arithmetic mean of such reading will closely approximate to an integral.

Thus we can write

$$F_G = \frac{\rho A_g \bar{V}_g^2}{g} + (\bar{P}_c - P_a) A_g \quad \dots \dots \dots (2)$$

where \bar{V}_g and \bar{P}_c are average values.

It can be shown this will reduce to the form

$$\frac{F_G}{A_g} = \frac{2J}{R} k_p \bar{P}_c (t - 1) + (\bar{P}_c - P_a) \quad \dots (3)$$

This is the form which has been used in the calculations which were computed in tabular form for ease of handling. Table I shows typical figures which were obtained during the flight tests.

2. With the front rake

Again equation (1) can be used, but it was found more convenient to use it in the form

$$\frac{F_G}{A_f 1} = \frac{\rho \bar{V}_g^2}{g} + (P_c - P_a)$$

The one dimensional theory for nozzles was assumed, thus

$$P_c = P_a \quad \text{or} \quad \frac{\bar{P}_{et}}{\left(\frac{\gamma + 1}{2}\right)^{\frac{\gamma}{\gamma - 1}}}$$

This has also been computed in tabular form and is shown in Table II.

TABLE I

Calculation of thrust and mass flow
from final nozzle rake 22

Test	32000 ft at 280 kts	25000 ft at 280 kts	15000 ft at 280 kts	10000 ft at 280 kts	5000 ft at 280 kts	400 ft at 280 kts
N rev/min corr	7942	7891	7287	7032	5714	6650
$\bar{T}_0 t = \bar{T}_0 t \text{ } ^\circ\text{K corr}$	810	820	746	714	661	659
$\bar{P}_e t \text{ lb/in}^2 \text{ corr}$	13.05	15.75	17.91	19.50	19.79	22.34
$\bar{P}_e \text{ lb/in}^2 \text{ corr}$	8.03	9.70	11.25	12.45	13.45	15.615
$P_a \text{ lb/in}^2$	3.93	5.40	6.22	10.03	12.20	14.45
$p = \frac{P_e t}{P_e}$	1.625	1.621	1.592	1.565	1.470	1.450
J_p	0.2659	0.2661	0.2615	0.2594	0.2562	0.2563
$\frac{\gamma}{\gamma - 1}$	3.879	3.880	3.810	3.780	3.740	3.740
$t = p \frac{\gamma - 1}{\gamma}$	1.1534	1.1327	1.130	1.126	1.1085	1.100
$\frac{2J}{R} \text{ (constant)}$	29.17					
$\frac{2J}{R} \text{ } \ln P_e (t - 1)$	8.31	10.00	11.15	11.23	10.9	11.73
$P_e - P_a \text{ lb/in}^2$	4.10	4.30	5.03	2.42	1.25	1.165
$F_G' / A_e \text{ lb/lb/in}^2$	12.71	14.5	14.10	14.30	12.15	12.345
$F_G' \text{ lb}$	3822	4405	4370	4200	3742	3952
FOR MASS FLOW						
$2gJ \text{ (constant)}$	90,150					
$V = \sqrt{2gJ C_p T_0 t \left(\frac{t - 1}{t} \right)}$	1511	1518	1423	1368	1225	1250
$\rho = \frac{1.5 P_e}{T_0 t} \times t$	0.01685	0.0201	0.0256	0.02945	0.0338	0.0391
$Q_e = \rho A_e V_e \text{ lb/s}$	54.43	65.3	77.9	86.2	68	103
$Q_F \text{ lb/s}$	0.524	0.95	0.93	0.93	0.804	0.87
$0.75 Q_F \text{ lb/s}$	0.393	0.71	0.700	0.70	0.60	0.65
$Q_1 = Q_e - 0.75 Q_F \text{ lb/s}$	53.8	64.6	77.2	85.5	67.4	102.35
Rake Drag lb	53	64	72.9	79	71	79
$F_G \text{ lb}$	3769	4341	4297	4321	3671	3875

TABLE II

Calculation of thrust and mass flow
from jet pipe rake

Test	20000 ft at 280 kts	25000 ft at 280 kts	15000 ft at 280 kts	10000 ft at 280 kts	5000 ft at 280 kts	400 ft at 280 kts
N rev/min corr	7942	7591	7287	7032	6714	6650
T_{5t} °K corr	810	820	746	714	661	659
P_{5t} lb/in ² corr	15.18	16.05	18.14	19.62	20.01	22.48
FOR CHOKING						
Cp	0.2653	0.2657	0.2610	0.2584	0.2550	0.2550
$\frac{\gamma}{\gamma - 1}$	3.870	3.875	3.805	3.770	3.720	3.720
γ	1.348	1.349	1.357	1.361	1.367	1.367
$\frac{\gamma + 1}{2} = t_c$	1.174	1.175	1.178	1.18	1.183	1.183
$P_c = t_c^{\frac{\gamma}{\gamma - 1}}$	1.86	1.866	1.865	1.865	1.870	1.870
FOR IMPINGE NOZZLE						
P_5 lb/in ²	7.08	8.59	9.72	10.52	12.20	14.45
P_a lb/in ²	3.95	5.40	8.22	10.03	12.20	14.45
Cp	-	-	-	-	0.2556	0.2558
$\frac{\gamma}{\gamma - 1}$	-	-	-	-	3.73	3.735
P_5 overall	-	-	-	-	1.64	1.555
t_5	1.174	1.175	1.178	1.18	1.142	1.126
T_5 °K	690	698	653	605	579	585
$\Delta T = T_{5t} - T_5$ °C	120	122	111	109	82	74
$\rho = \frac{1.2 P_5}{T_5}$	0.0154	0.01646	0.02305	0.0261	0.0316	0.0370
$V^2 \times 10^{-6}$	2.87	2.92	2.65	2.54	1.39	1.77
$P_5 - P_a$ lb/in ²	3.15	3.19	1.5	0.49	0	0
$\frac{FV}{A_f^1} = \frac{\rho V^2}{g}$ lb/lb/ft ²	1373	1675	1905	2060	1855	2070
$\frac{F_P}{A_f^1} = 144(P_5 - P_a)$ lb/lb/ft ²	454	459	216	70.5	0	0
F_G/A_f^1 lb/lb/ft ²	1027	2134	2,2121	2130.5	1855	2070
A_f^1 ft ²	2.04	2.04	2.04	2.04	1.945	1.950
F_G lb	5727	4355	4350	4345	3608	4040
$Q_5 = \rho A_f^1 V$ lb/s	53.2	61.3	76.6	81.8	84.5	96.0
Q_P lb/s	0.824	0.95	0.93	0.93	0.804	0.87
$0.75 \times Q_P$	0.62	0.71	0.70	0.70	0.60	0.65
$Q_1 = Q_5 - 0.75 Q_P$ lb/s	52.58	63.50	75.9	84.1	83.9	95.35

Appendix III

Thrust measurement in flight

Derivation of ambient temperature and pressure

Ambient pressure

An altimeter position error as determined from A. and A.E.E. Report No. A.A.E.E./86/1 dated 5th April, 1951, was applied to the mean value of recorded heights for one particular level. Since all flights were carried out with the altimeter sub scale set to 1,013.2 mbs, the ICAN pressure equivalent of the true altitude gives ambient pressure (P_a).

N.B. Since the static sides of all differential pressure gauges used on the rakes were connected to the aircraft static system, the pressure equivalent of altitude, without position error applied, was used to obtain absolute values of pressure from gauge values.

Ambient temperature

Ambient air temperature was derived from the reading of a type IT-3-2 impact bulb in the following manner.

A mean value of indicated air speed was derived from the recorded values of air speed for one particular altitude and nominal air speed. From a knowledge of the all up weight of the aircraft a position error correction was obtained from A. and A.E.E. Report No. A.A.E.E./86/1. Application of position error correction and compressibility error correction were made to the mean indicated air speed to give equivalent air speed.

Let V = true air speed
 V_e = equivalent air speed
 T_a = ambient air temperature
 T_{at} = total ambient temperature as recorded by IT-3-2 bulb
 k = temperature recovery factor
 T = standard temperature at ICAN altitude
 δ = standard relative density at ICAN altitude
 δ_1 = true relative density at ICAN altitude
 T = temperature difference $T_{at} - T_a$.

Then for an adiabatic process

$$\Delta T = \frac{V^2}{2gJ k_p} \quad \text{and assuming recovery factor } k$$

$$\Delta T = k \frac{V^2}{2gJ k_p}$$

which can be written

$$\Delta T = k \left(\frac{V}{100} \right)^2 \quad \text{with } V \text{ in m.p.h.} \quad \dots (1)$$

$$V = \frac{V_c}{\sqrt{\delta_1}} \quad \text{and at a given pressure level}$$

$$\frac{1}{T_a \delta_1} = \frac{1}{T \delta}$$

$$\therefore V = \frac{V_c}{\sqrt{\frac{T \delta}{T_a}}} \quad \dots \dots \dots (2)$$

Substituting (2) in equation (1) gives

$$\Delta T = T_{a_t} - T_a = k \left(\frac{V_c}{100} \right)^2 \frac{T_a}{T \delta}$$

or

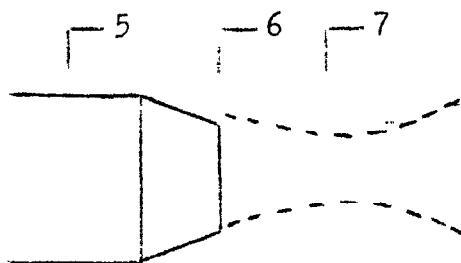
$$T_a = \frac{T_{a_t}}{1 + k \left(\frac{V_c}{100} \right)^2 \frac{1}{\delta T}}$$

.. value of k = 0.8 was used throughout.

Appendix IV

Thrust measurement in flight

Discharge from a jet pipe



Consider the diagram which represents the flow at exit from a jet pipe. It is assumed that when the critical pressure ratio over the nozzle is reached the throat is actually downstream of the physical nozzle throat, i.e. at plane 7 instead of plane 6.

Now if the system is choking the Mach number will be unity at plane 7. It is shown below that even though the system is choked it is possible for a limited increase in the ratio of $P_5 t/P_6$ to occur with an increase in $P_5 t/P_a$.

Assume that the following conditions are applicable:-

$$A_7 = 1.0 \qquad A_6 = 1.05 \qquad A_5 = 1.10$$

Thus

$$M_7 = 1.0 \qquad M_6 = 0.8 \qquad M_5 = 0.706$$

And if

$$P_5 t = P_6 t = P_7 t$$

$$P_5 t/P_7 = 1.862 \qquad P_5 t/P_6 = 1.502 \qquad P_5 t/P_5 = 1.58$$

Now if the overall pressure ratio $P_5 t/P_a$ is increased, there will be an increase in the nozzle discharge coefficient which can be regarded as an effective increase in the area in plane 7. Also A_6 will increase due to a thinning of the boundary layer.

Let us now assume that due to an increase in $P_5 t/P_a$ the areas will have changed to

$$A_7 = 1.02 \qquad A_6 = 1.06 \qquad A_5 = 1.1$$

which based upon

$$A_7 = 1.0$$

$$A_7 = 1.0 \qquad A_6 = 1.04 \qquad A_5 = 1.078$$

Thus

$$M_7 = 1.0 \qquad M_6 = 0.822 \qquad M_5 = 0.738$$

And

$$P_5 t/P_7 = 1.862 \qquad P_5 t/P_6 = 1.542 \qquad P_5 t/P_5 = 1.42$$

Thus due to an increase in overall nozzle pressure ratio an increase in the ratio of total head to static pressure has been experienced in the plane of the final nozzle although the system has remained choked throughout.

This effect can be seen in Figure 14 where $P_6 t/P_5$ has been plotted against overall nozzle pressure ratio. It will be noted that $P_6 t/P_5$ does not reach a maximum until $P_5 t/P_a$ has reached about 2.3. It also shows that $P_6 t/P_5$ never reaches the theoretical value of 1.86, the reason being shown in Figures 3 and 8 which show the static pressure distribution. Thus it could therefore be argued that this high static pressure is due to the effective nozzle throat being in fact downstream of the throat of the physical nozzle.

THRUST MEASUREMENT IN FLIGHT.
ARRANGEMENT OF RAKES IN JET PIPE.

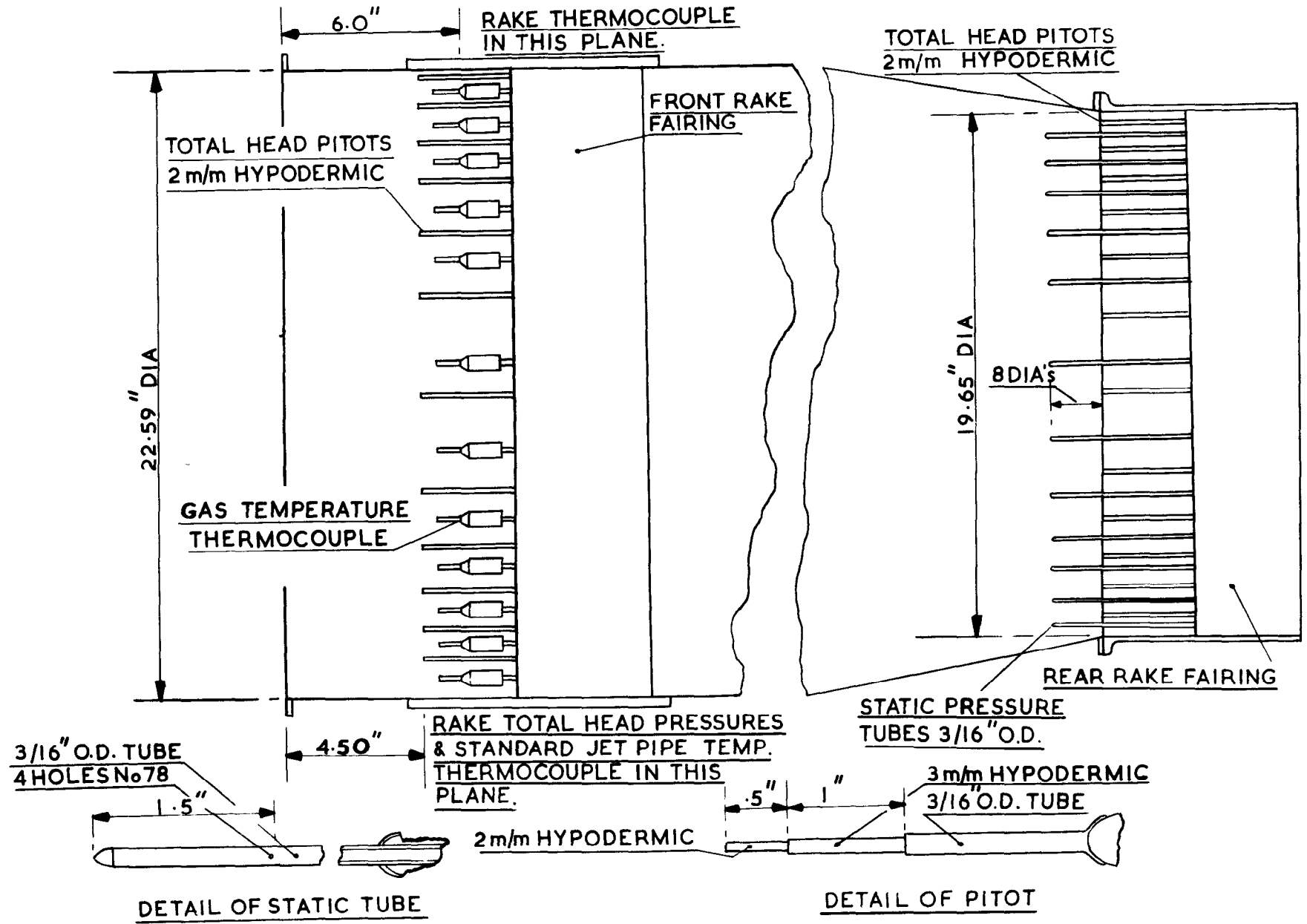
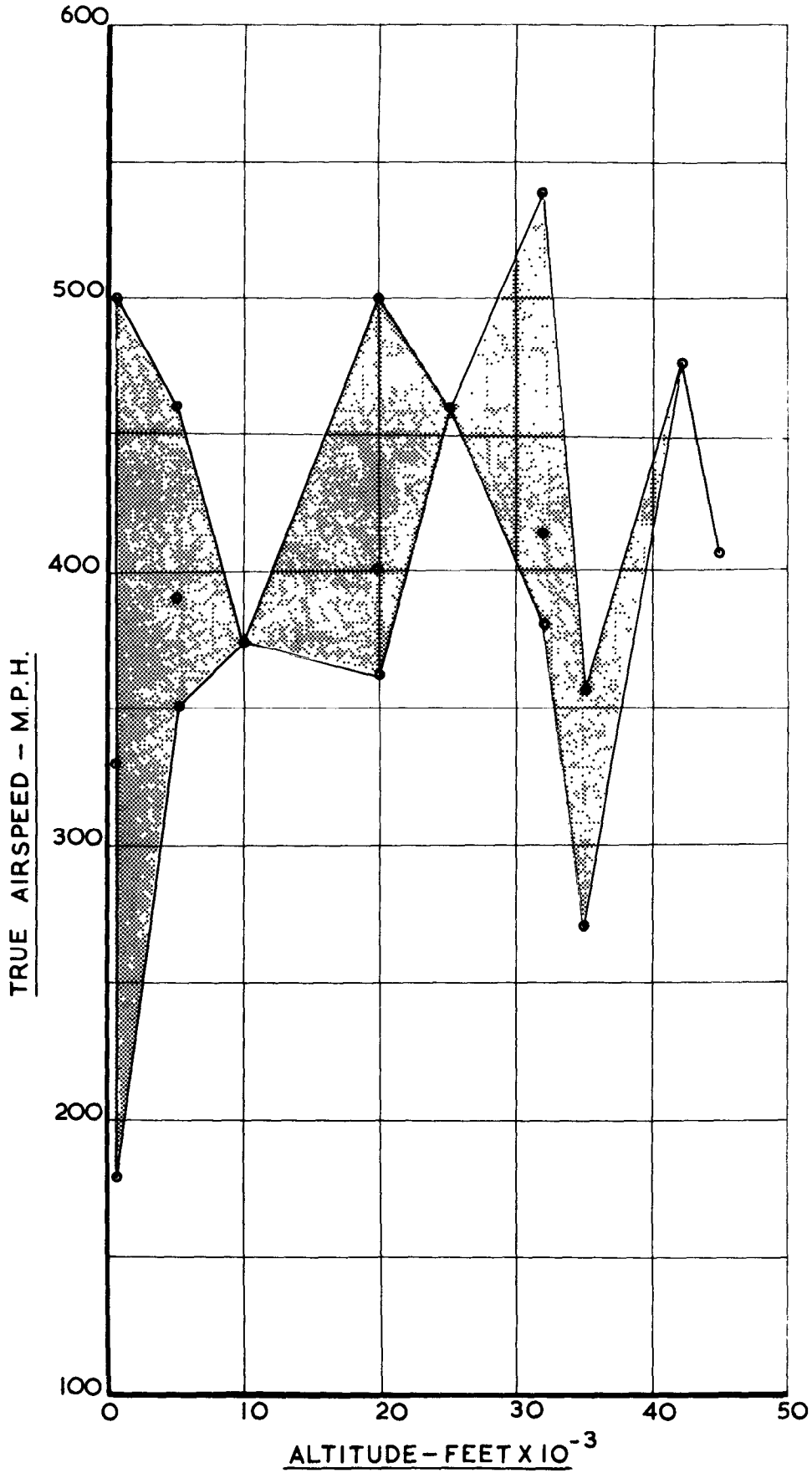


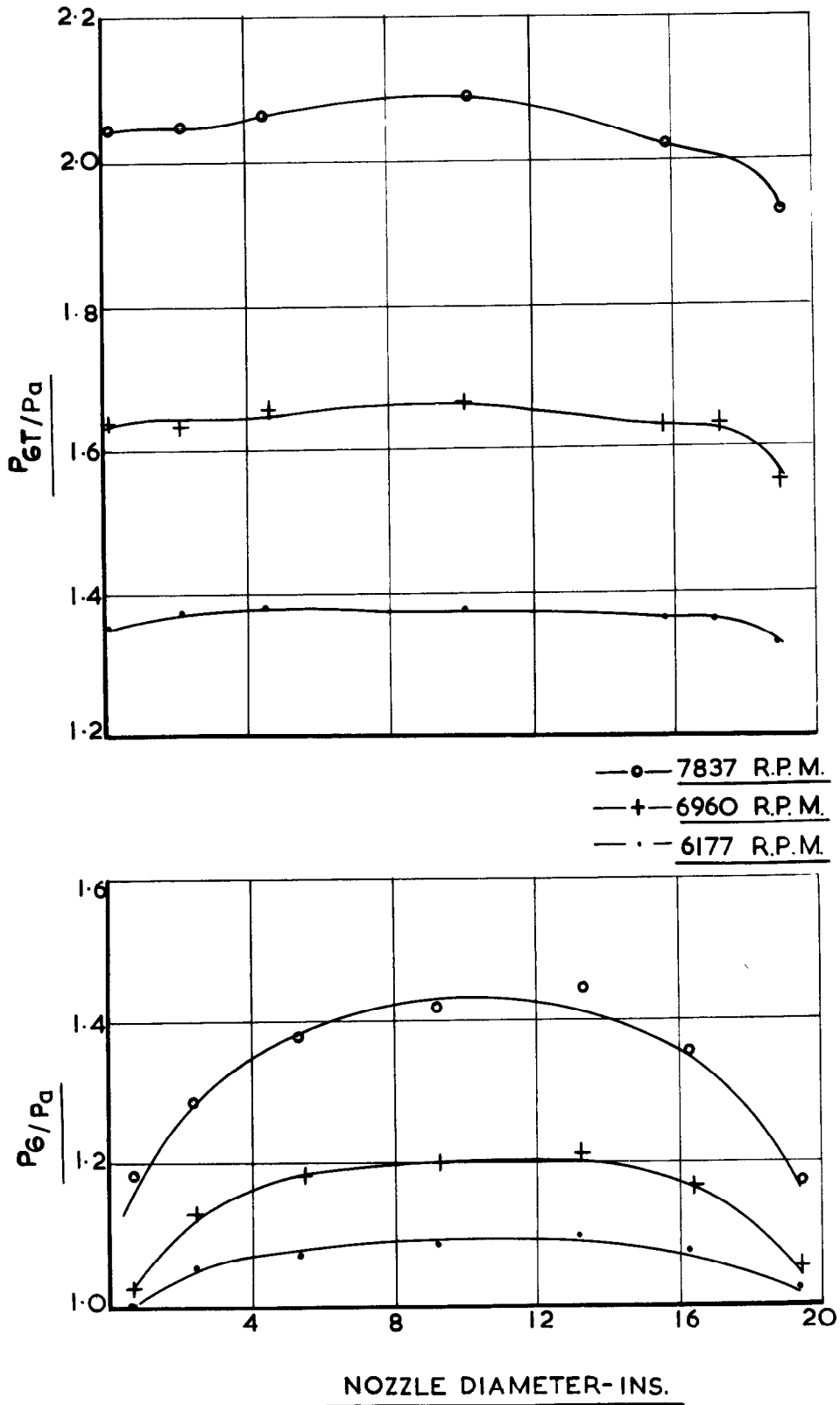
FIG. 1.

FIG.2.



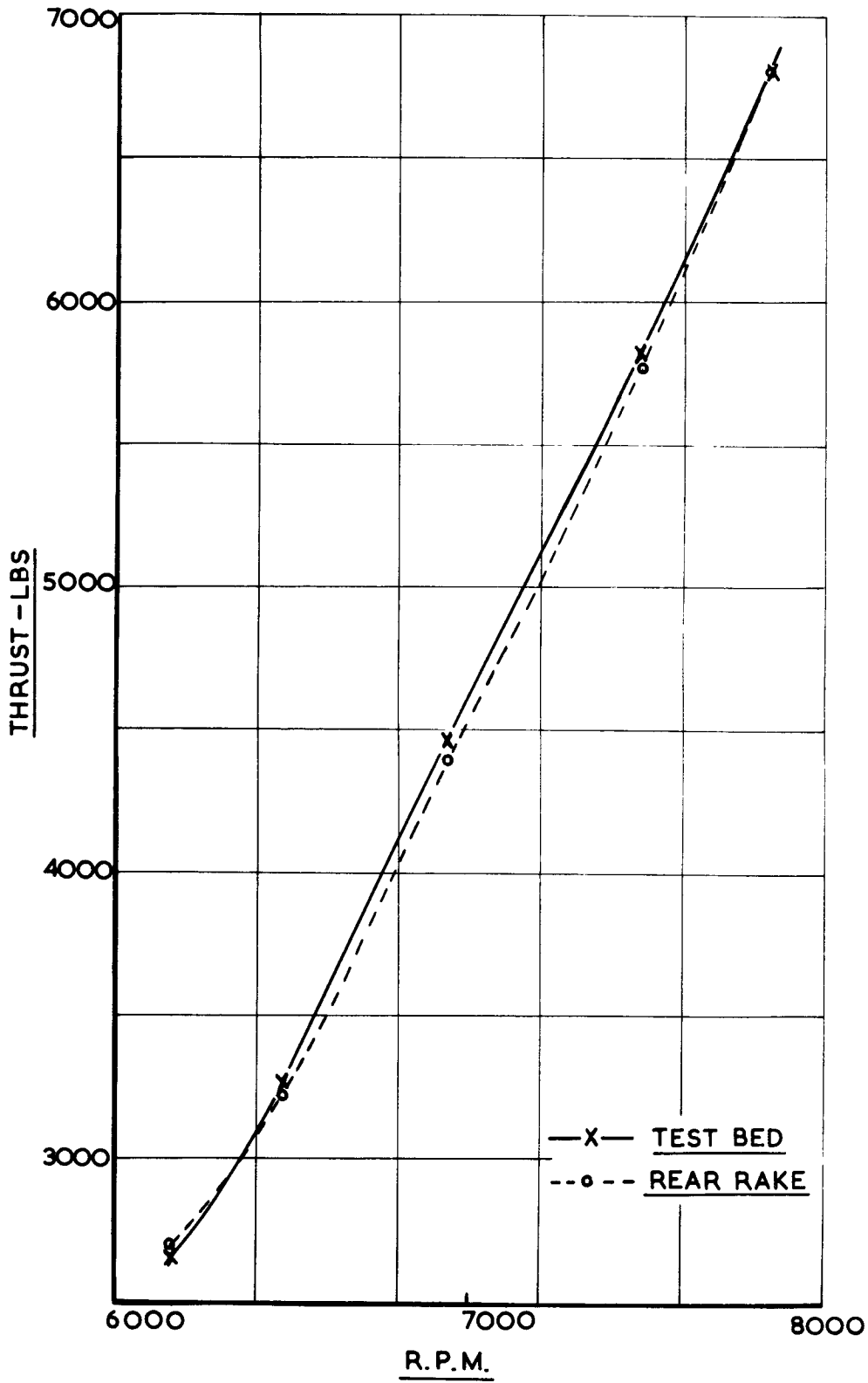
THRUST MEASUREMENT IN FLIGHT.
DIAGRAMMATIC REPRESENTATION OF SPEEDS
& ALTITUDES COVERED DURING FLIGHT TRIALS.

FIG.3.



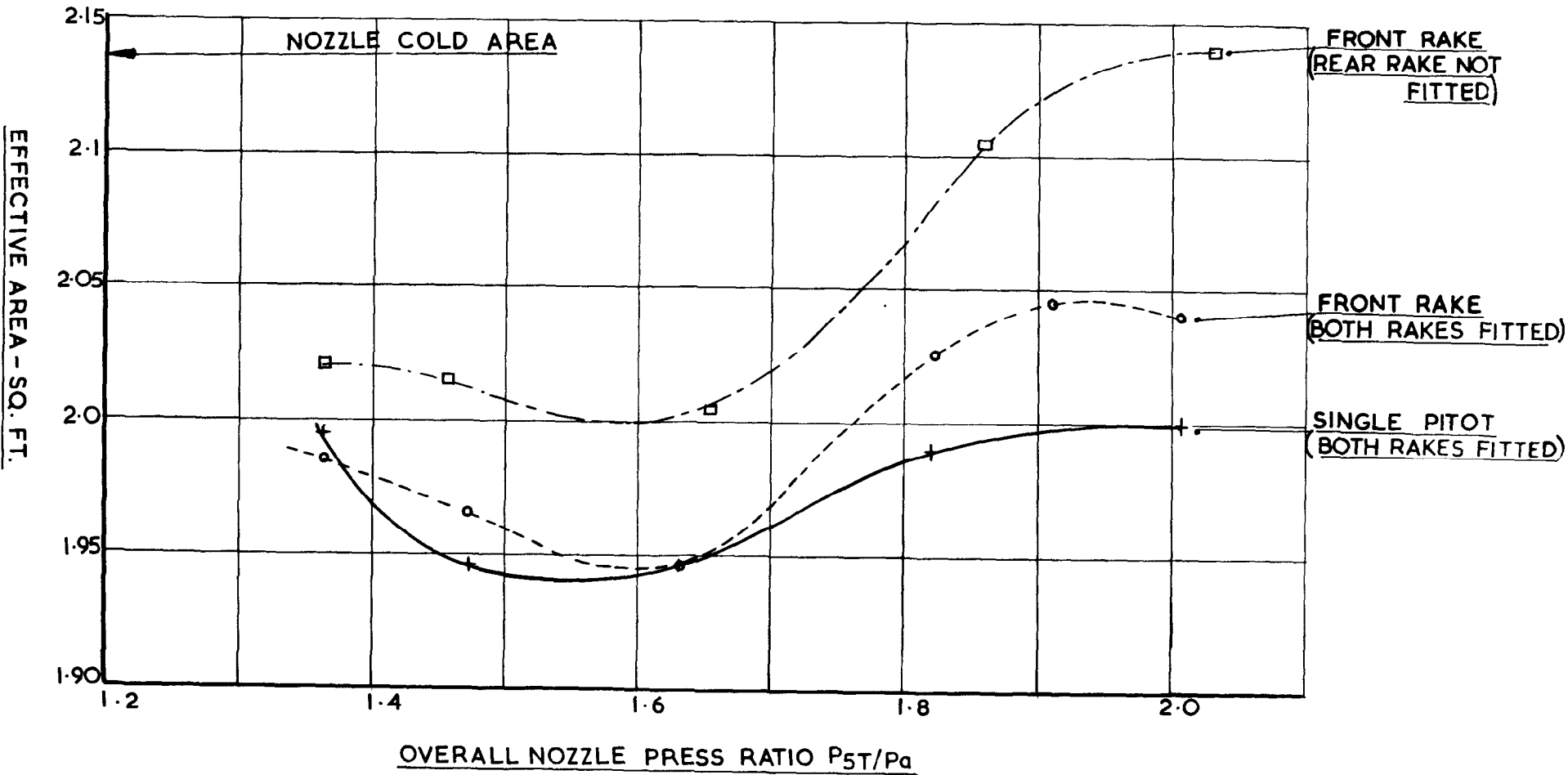
THRUST MEASUREMENT IN FLIGHT.
TYPICAL PRESSURE DISTRIBUTION ACROSS
FINAL NOZZLE. TEST BED RESULTS.

FIG.4.

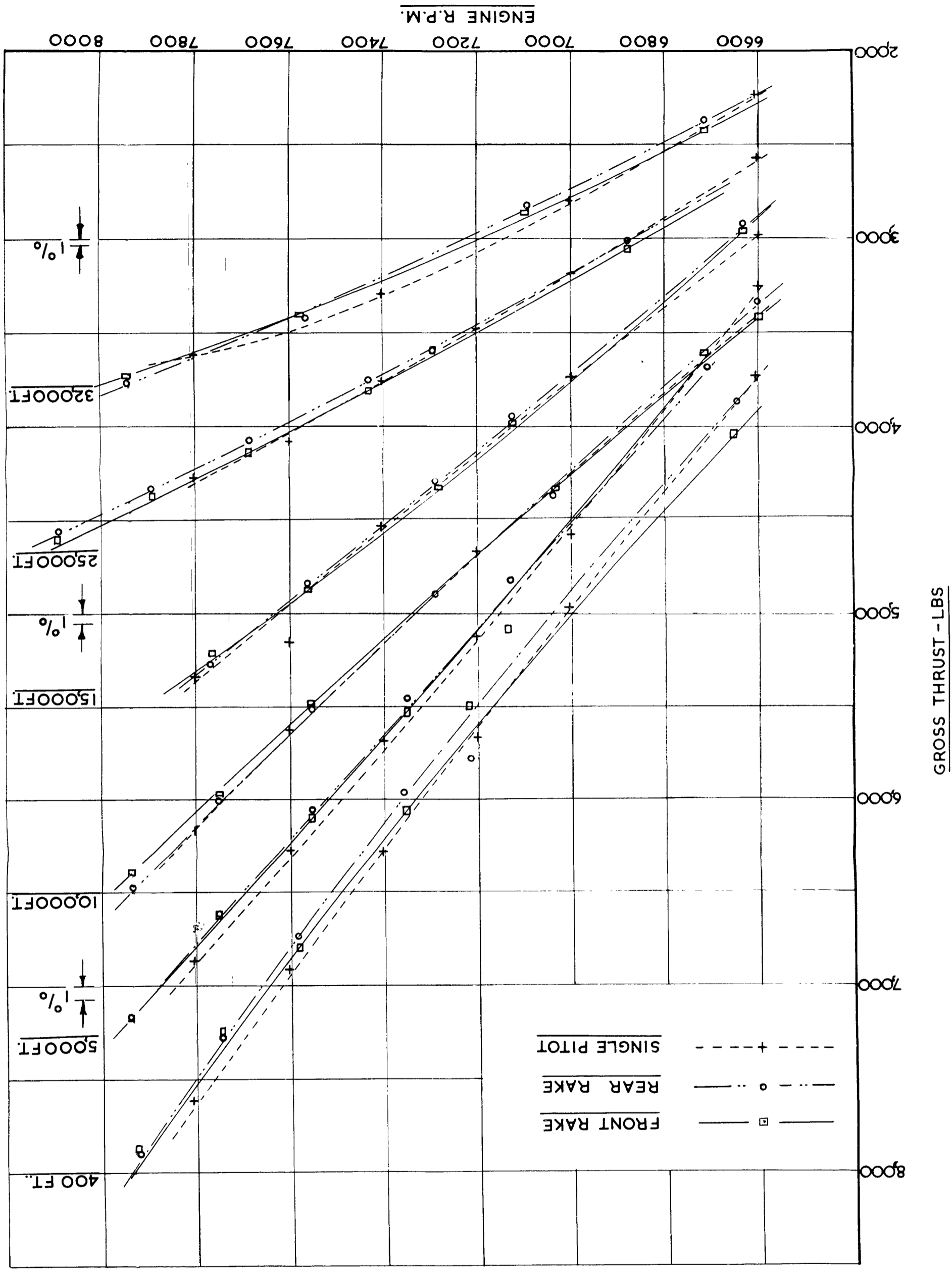


THRUST MEASUREMENT IN FLIGHT.
TEST BED MEASURED THRUST AND
CALCULATED REAR RAKE THRUST.

FIG.5.

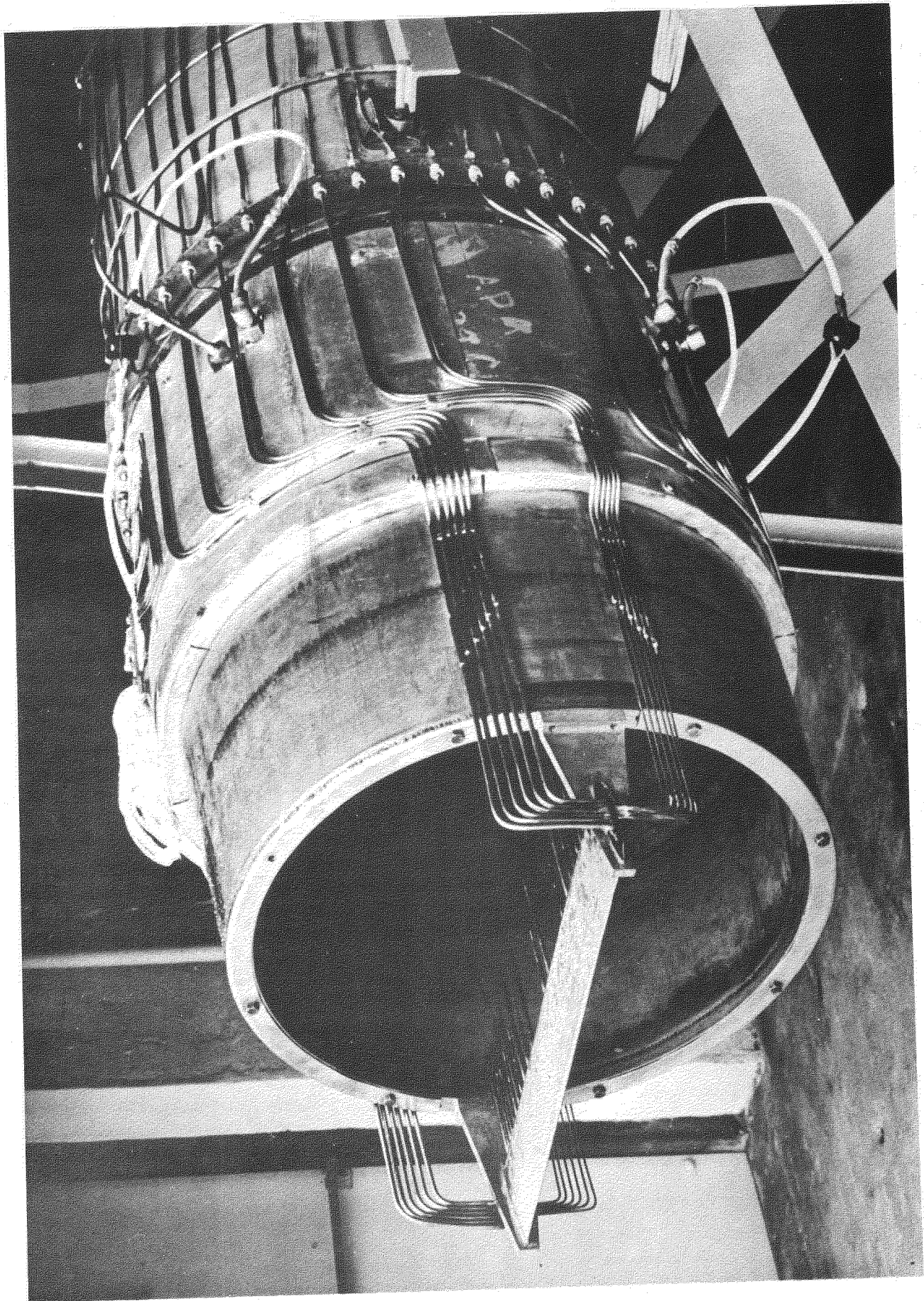


THRUST MEASUREMENT IN FLIGHT.
EFFECTIVE AREA CALIBRATION CURVES.



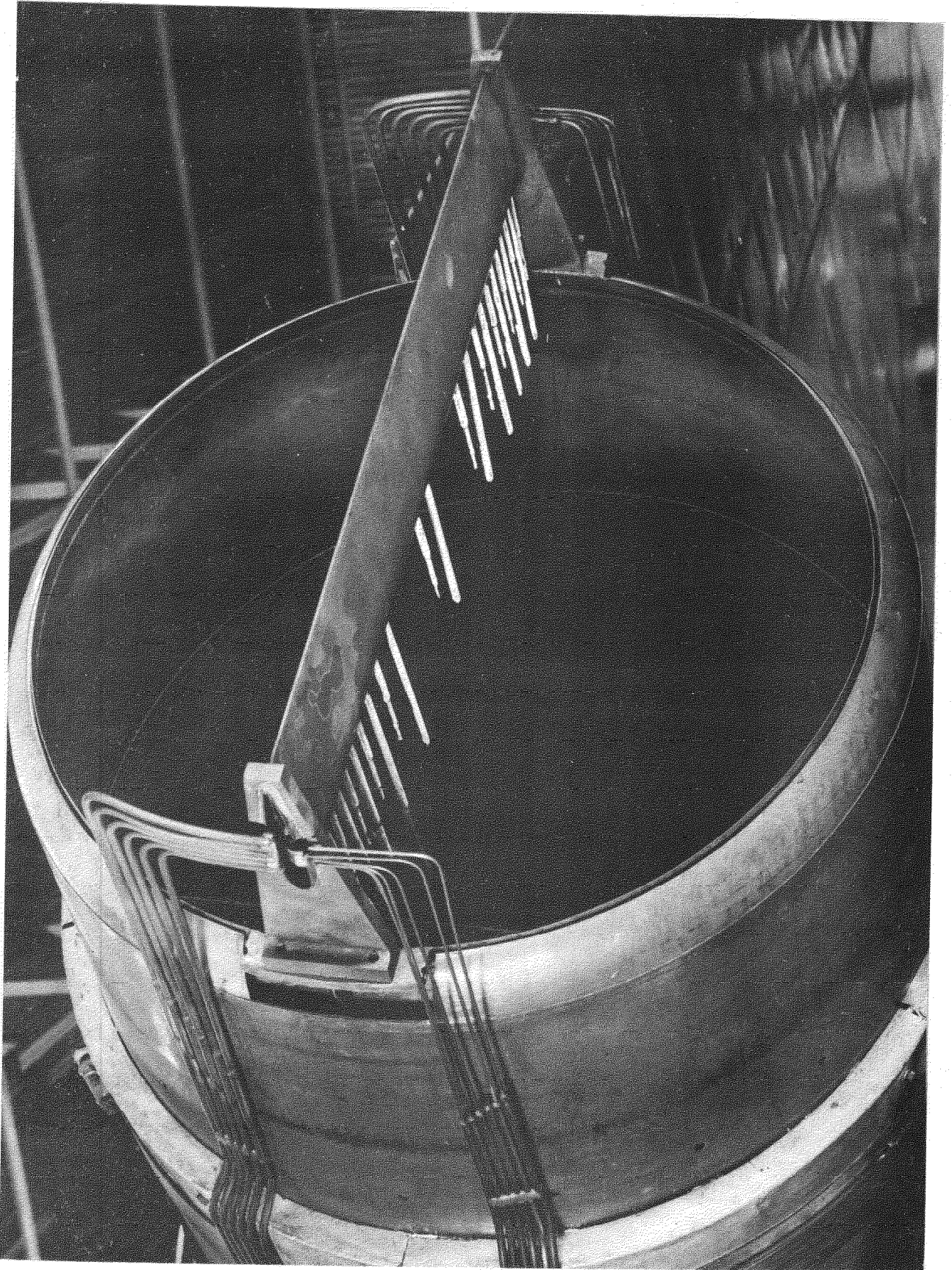
THRUST MEASUREMENT IN FLIGHT.

TYPICAL THRUST V. R.P.M. CURVES OBTAINED DURING FLIGHT TRIALS.

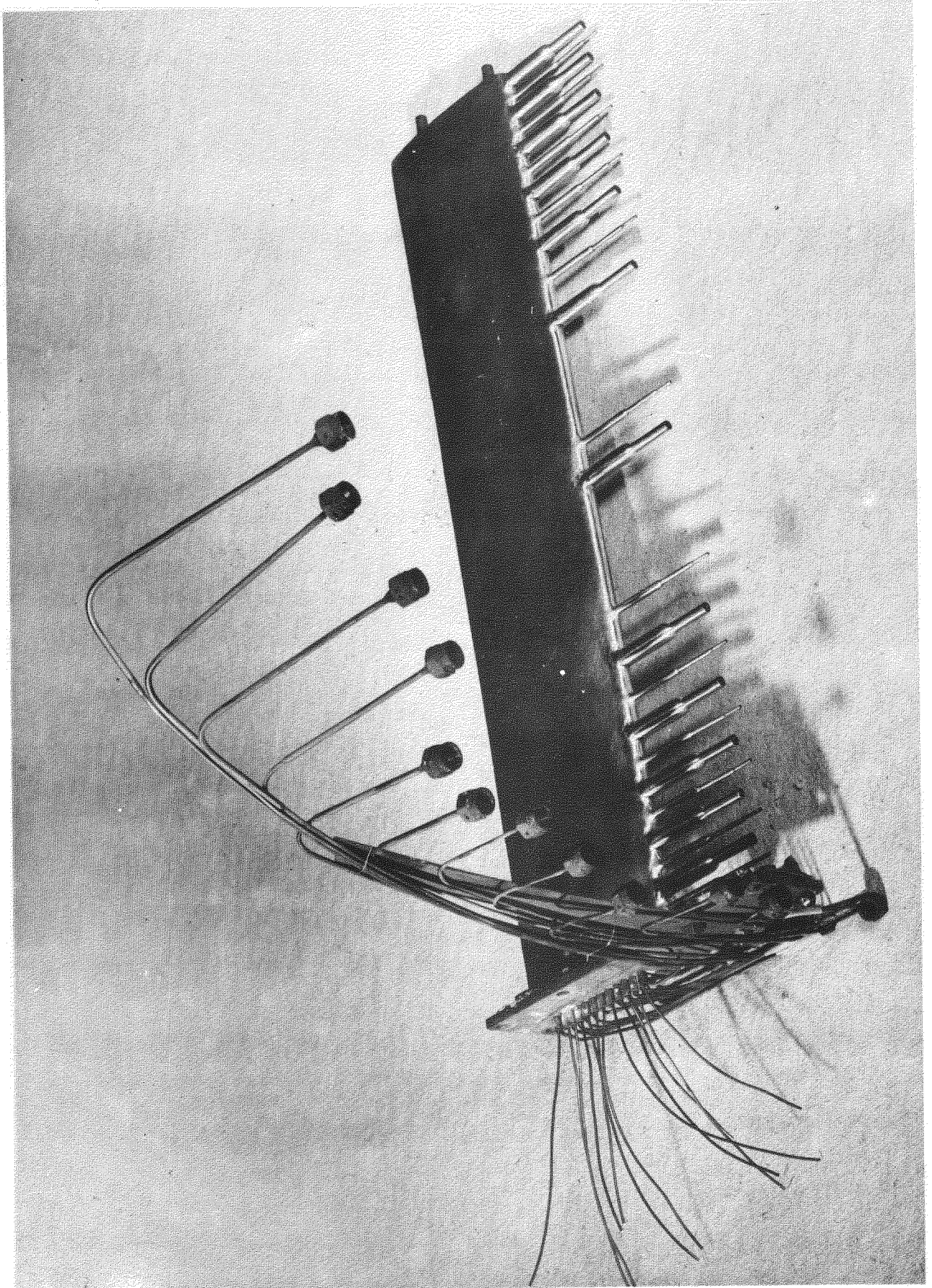


THRUST MEASUREMENT IN FLIGHT.

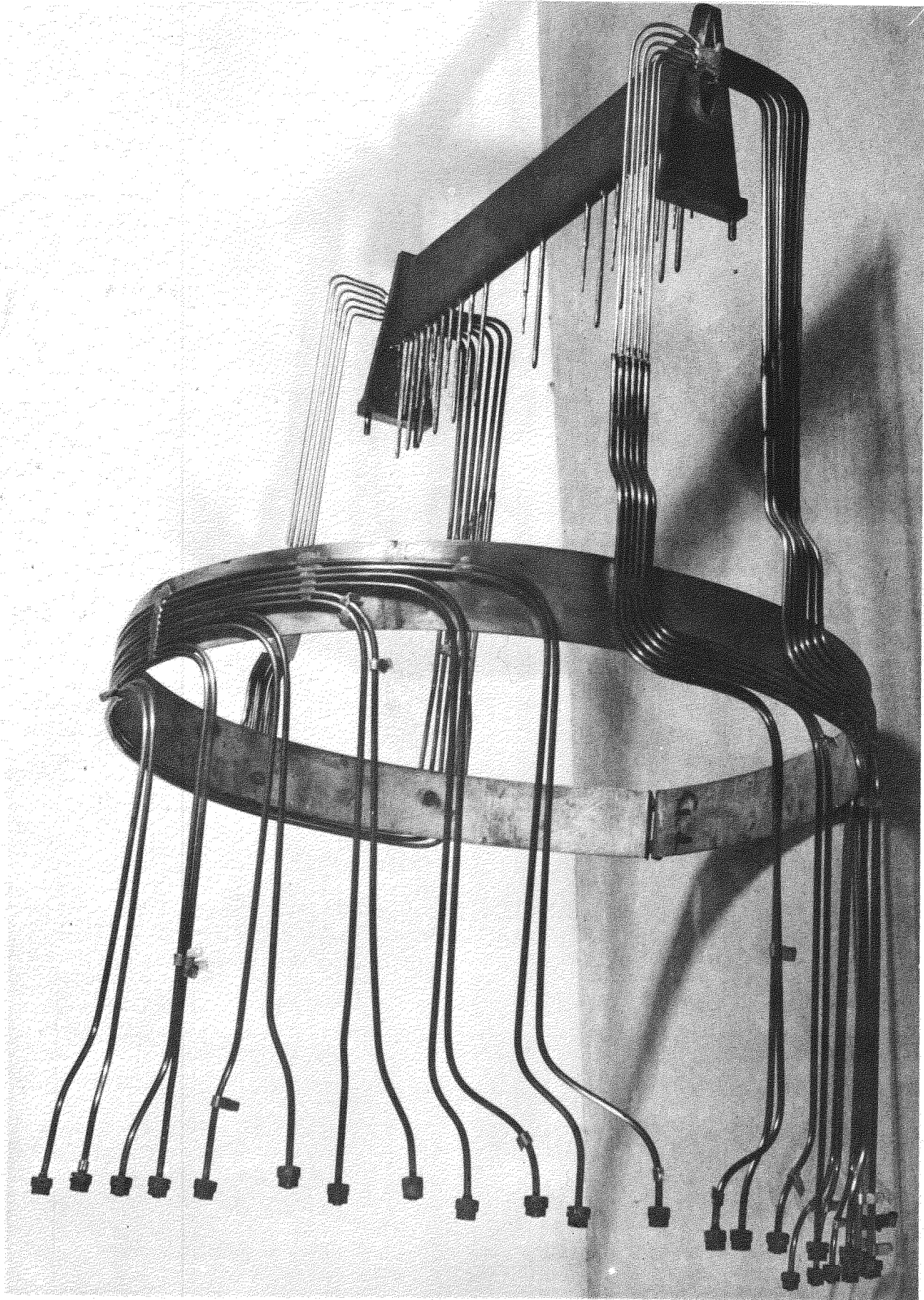
FINAL NOZZLE PRESSURE RAKE.



THRUST MEASUREMENT IN FLIGHT.
FINAL NOZZLE RAKE AFTER FLIGHT
TESTS.

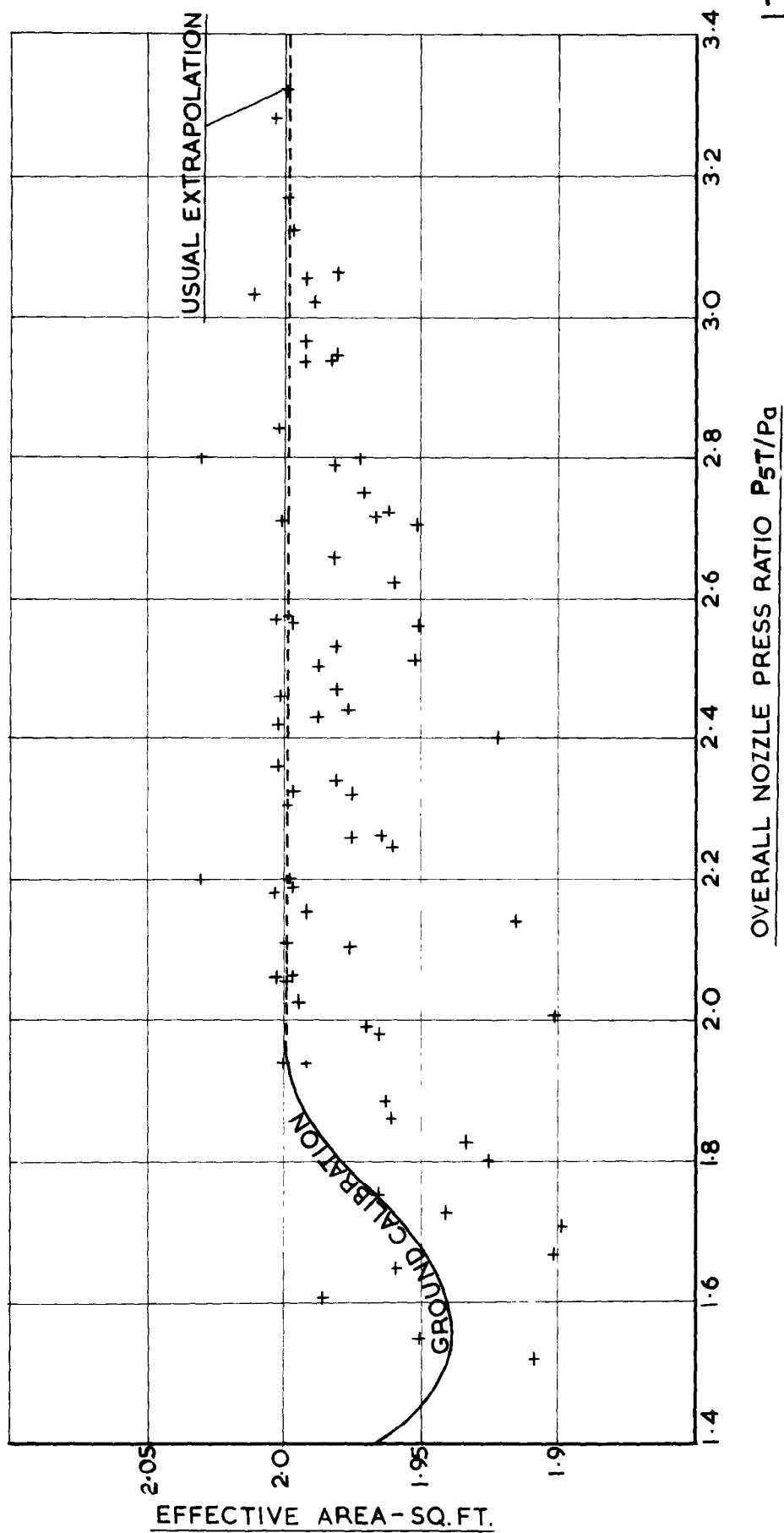


THRUST MEASUREMENT IN FLIGHT
FRONT RAKE AFTER REMOVAL & REPAIR.



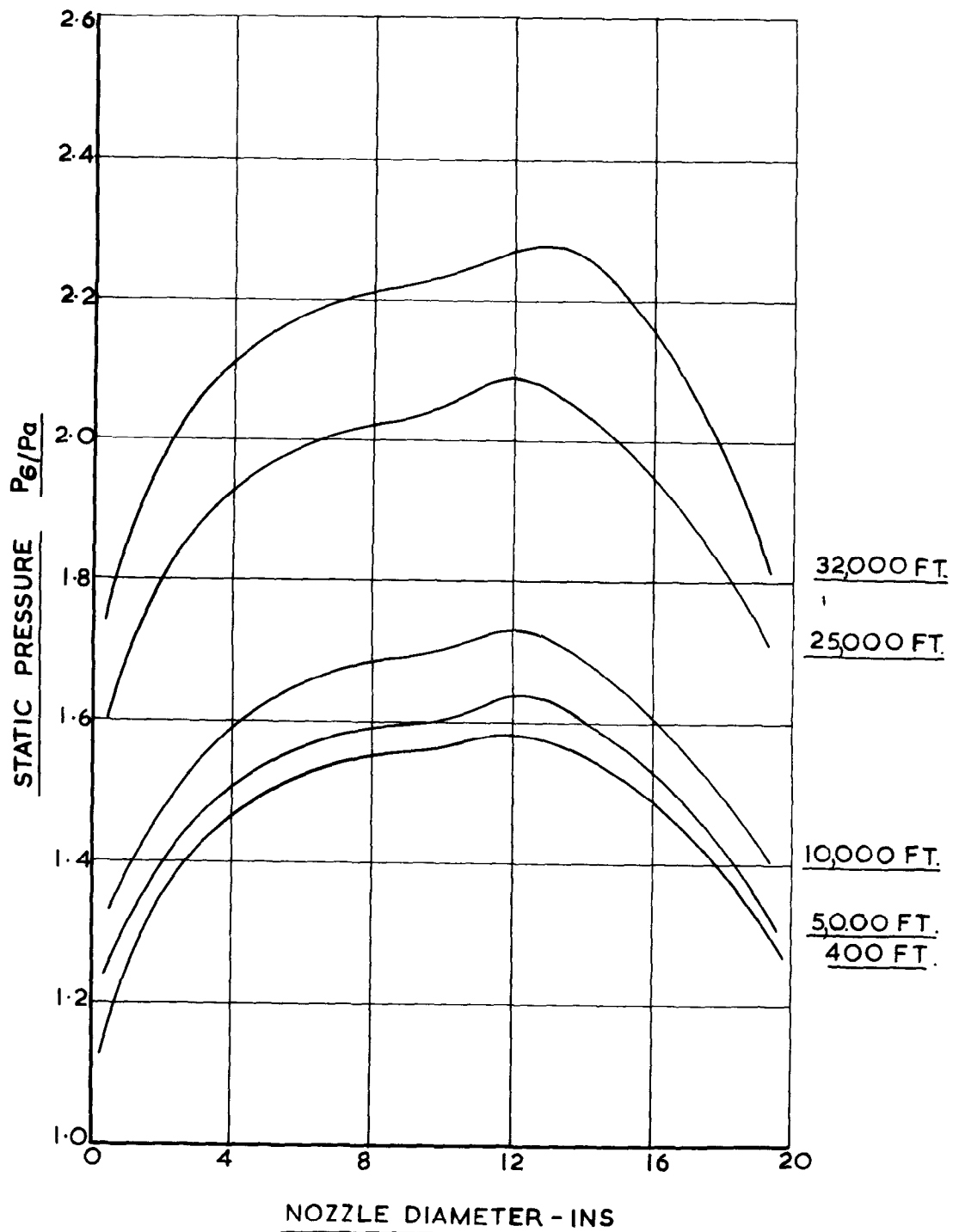
THRUST MEASUREMENT IN FLIGHT
REAR RAKE AFTER REMOVAL & REPAIR.

FIG. 7.



THRUST MEASUREMENT IN FLIGHT.
SINGLE PITOT EFFECTIVE AREA COMPUTED
FROM FLIGHT RESULTS.

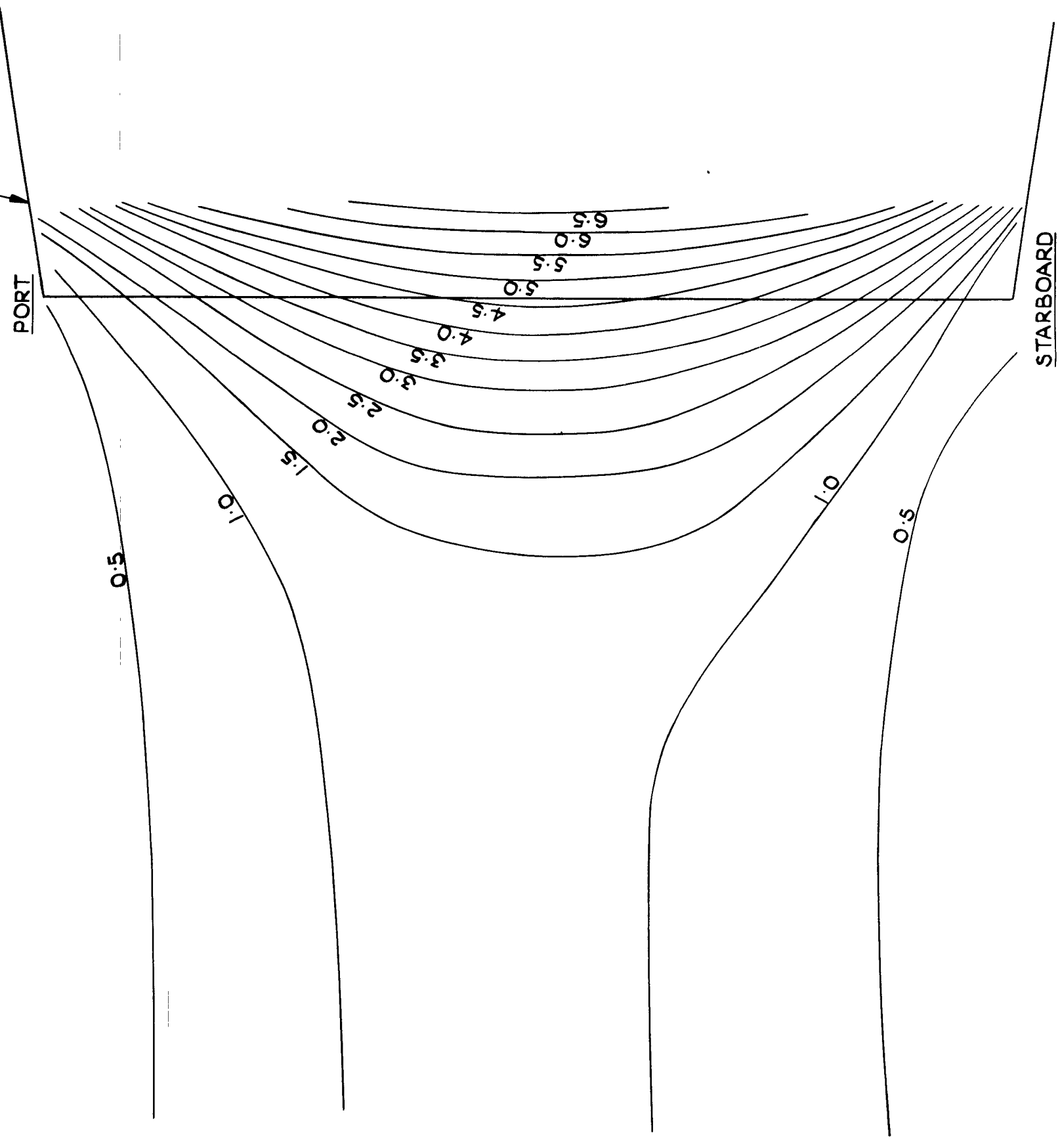
FIG. 8.



THRUST MEASUREMENT IN FLIGHT
STATIC PRESSURE DISTRIBUTION
ACROSS FINAL NOZZLE.

NOZZLE OUTLINE

FIGURES SHOW PRESSURE IN INS. OF MERCURY

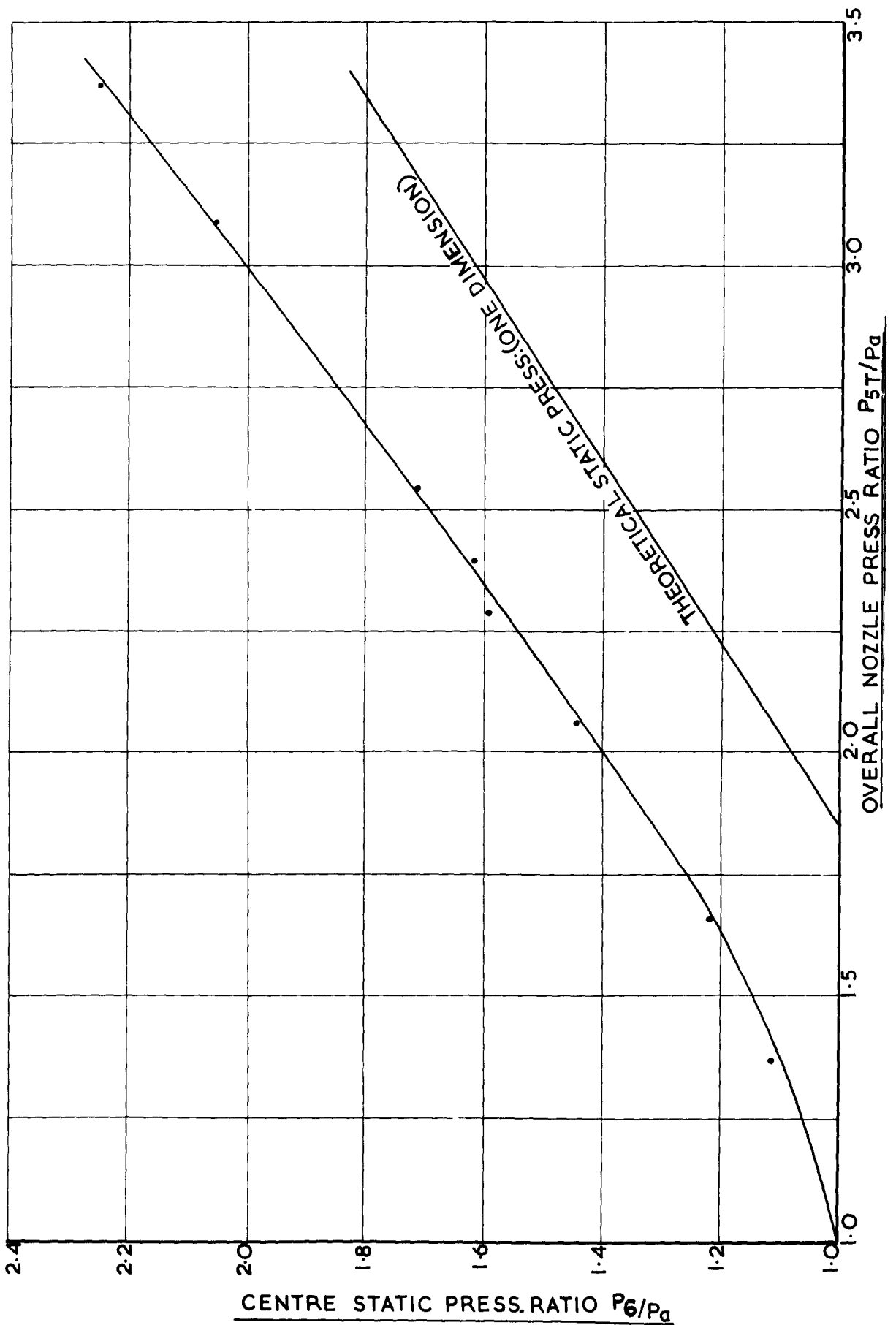


CONTOUR LINES OF STATIC PRESSURE IN HORIZONTAL PLANE THROUGH FINAL NOZZLE

DERWENT V ENGINE No. 3456 CORRECTED SPEED 14,750 R.P.M.

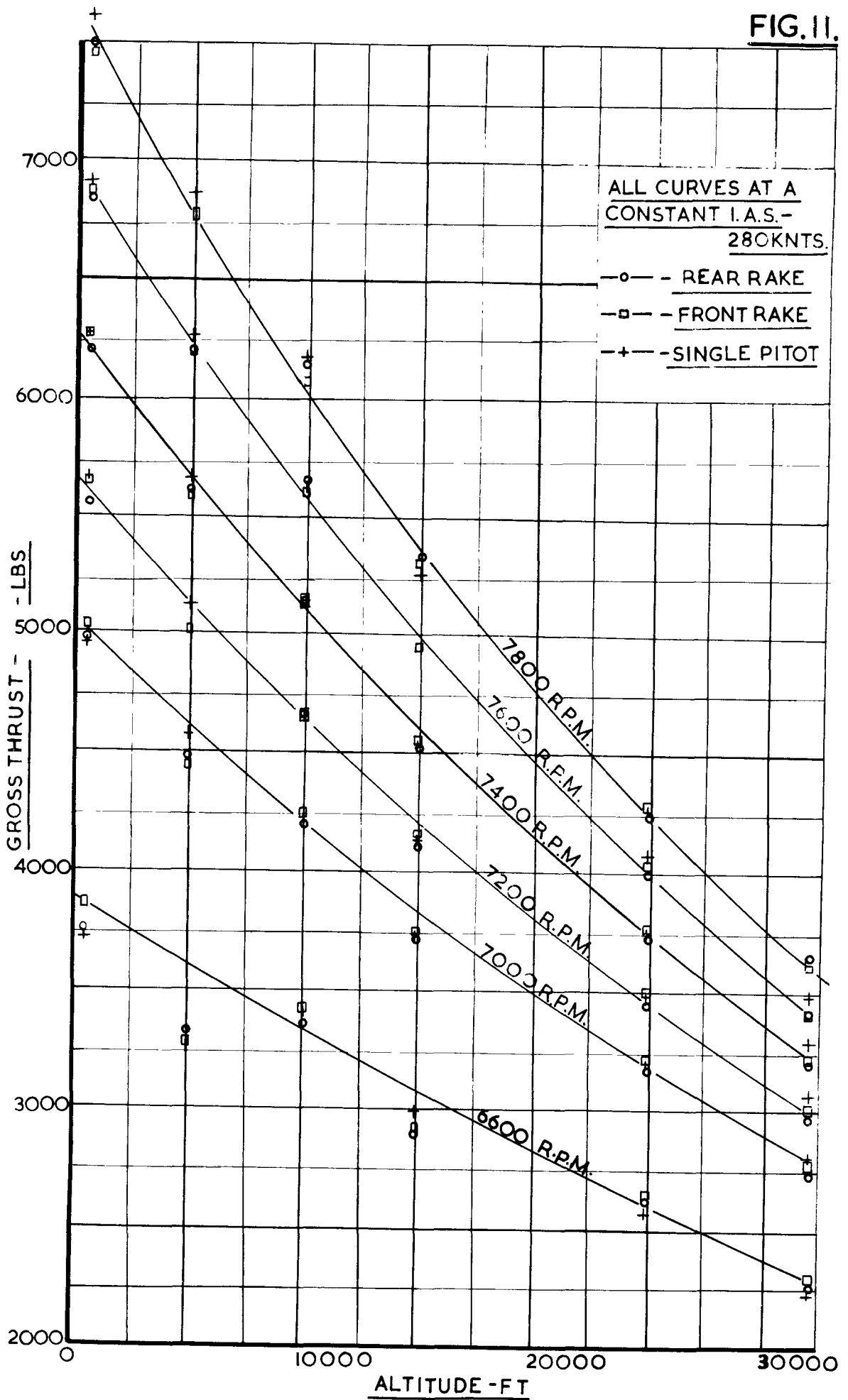
SCALE 1/2 FULL SIZE

FIG.10.



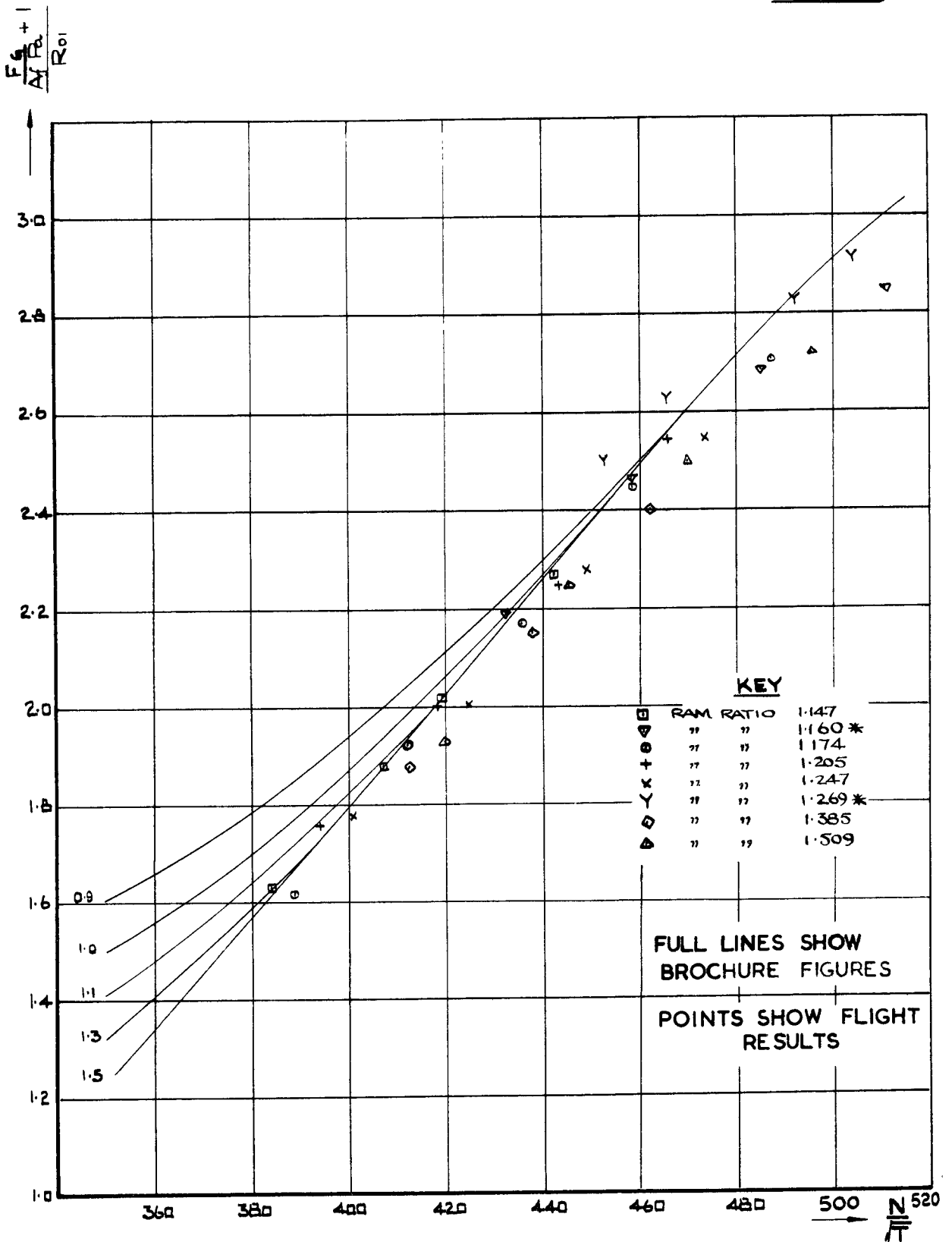
THRUST MEASUREMENT IN FLIGHT.
CENTRE STATIC PRESSURE RATIO V. OVERALL
NOZZLE PRESSURE RATIO.

FIG. II.



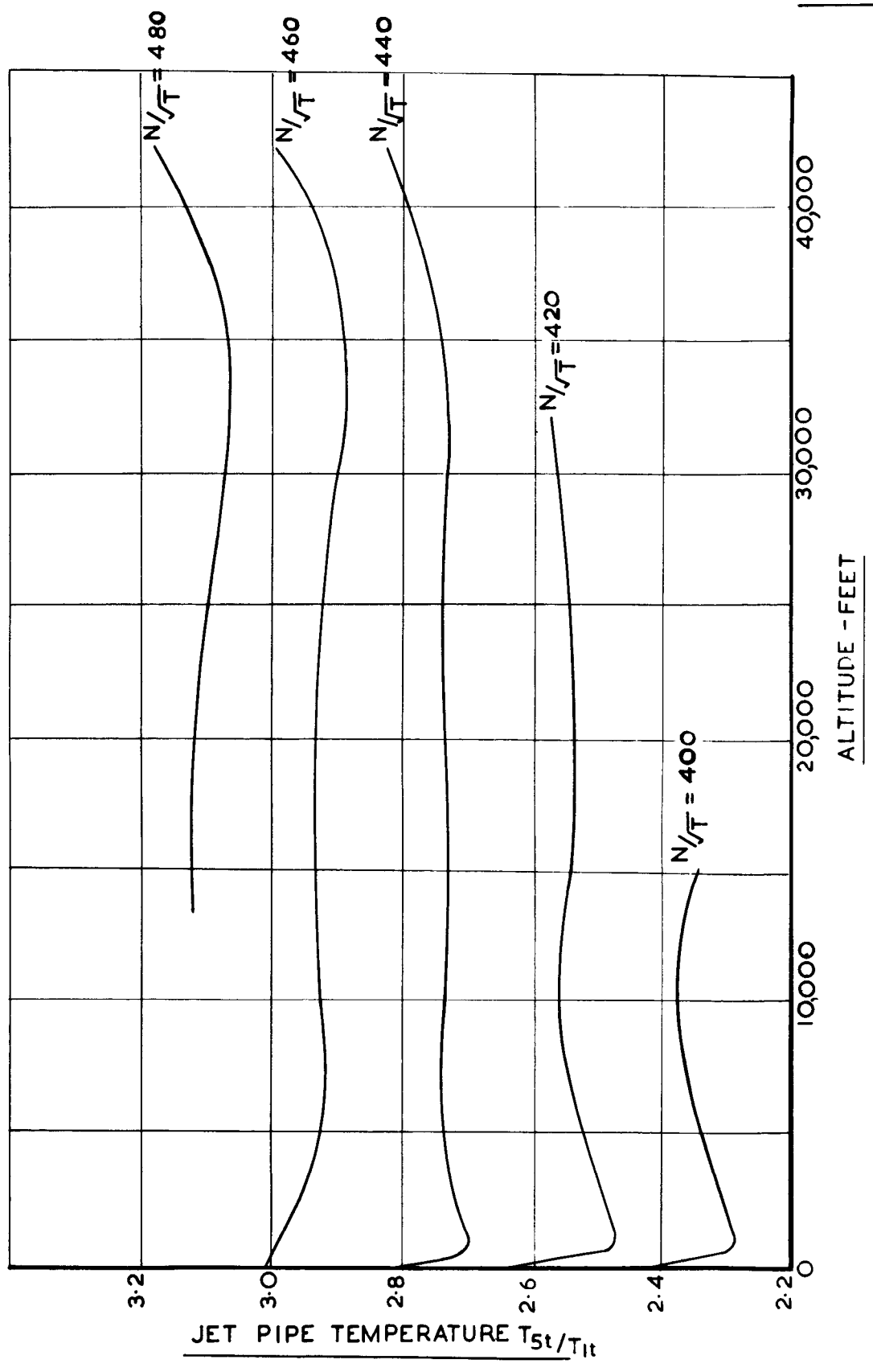
THRUST MEASUREMENT IN FLIGHT.
THRUST V ALTITUDE CHART.

FIG. 12.



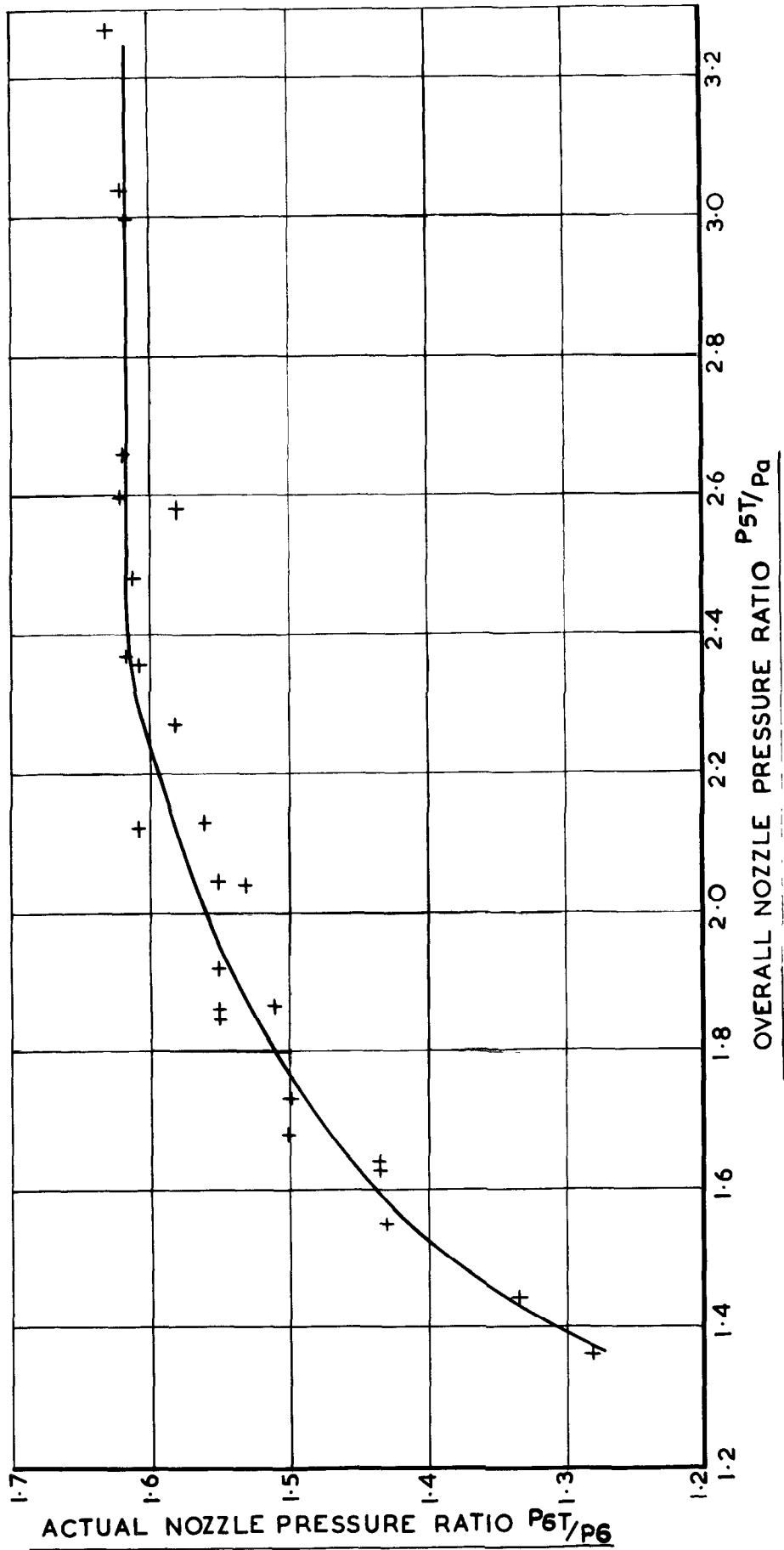
THRUST MEASUREMENT IN FLIGHT
NON-DIMENSIONAL PLOT OF THRUST V R.P.M.
SHOWING CORRELATION OF THEORETICAL
FIGURES TO ACTUAL RESULTS

FIG.13.



THRUST MEASUREMENT IN FLIGHT
JET PIPE TEMPERATURE V. ALTITUDE.

FIG.14.



THRUST MEASUREMENT IN FLIGHT.
ACTUAL NOZZLE PRESSURE RATIO
V. OVERALL NOZZLE PRESSURE RATIO.

© *Crown copyright* 1960

Printed and published by
HER MAJESTY'S STATIONERY OFFICE

To be purchased from
York House, Kingsway, London w.c.2
423 Oxford Street, London w.1
13A Castle Street, Edinburgh 2
109 St. Mary Street, Cardiff
39 King Street, Manchester 2
50 Fairfax Street, Bristol 1
2 Edmund Street, Birmingham 3
80 Chichester Street, Belfast 1
or through any bookseller

Printed in England